ABSTRACT

Emily A. Wright. ROLE OF COLD FRONTS IN SOUTH AMERICAN MONSOON ONSET (under the direction of Dr. Rosana Nieto Ferreira) Department of Geography, July, 2010.

During the austral spring, the interactions between the southward-moving intertropical convergence zone with cold fronts that progress equatorward contribute to the complexity of the timing and regional differences in South American Monsoon onset. This thesis studied the impact of cold fronts on the onset of the South American monsoon. Previous studies have shown that cold fronts undergo a seasonal transition in structure, intensity and propagation. In fact, whereas wintertime cold fronts bring relatively little rainfall but strong temperature anomalies to South America, summertime cold fronts affect the rainfall patterns well into the tropical portions of the continent but cause very small changes in temperature. Cold fronts are the dynamical trigger of monsoon onset in at least some regions of South America.

In this study the 1979-2007 the National Center for Environmental Prediction and the National Center for Atmospheric Research reanalysis data (NCEP/NCAR) and Global Precipitation Climatology Project (GPCP) data are used to produce a composite analysis of the dynamic and thermodynamic structures, intensity and propagation of cold fronts that occur before ("pre-onset), during ("onset), and after ("post-onset") monsoon onset in the SACZ region. Those composites are used to study the effect of cold fronts on the abrupt onset of the monsoon season in the region of the South Atlantic convergence zone (SACZ).

The "pre-onset", "onset", and "post-onset" composites showed differences in speed and propagation of the cold fronts. In the "pre-onset" composites, cold fronts passed through South America quickly and did not reach the SACZ region. The "onset" composites showed cold fronts moving through the SACZ region and becoming stationary, bringing precipitation to the region. The precipitation in the region due to cold fronts is an indicator of the abrupt and dynamic onset

in the region. Therefore at the time of “onset”, there is a radical change in the structure and propagation of cold fronts propagating through South America that triggers monsoon onset in the SACZ region.

Years with normal, early and late onsets were compared to understand how thermodynamic changes, such as volumetric soil moisture, and sensible and latent heat fluxes, contribute to monsoon onset in the region. Quick changes in the thermodynamic variables right before onset in the SACZ region indicate that there is a fast onset triggered by cold fronts. In the WR, since there is a slow change in the thermodynamic variables before onset, WR onset does not seem to be associated with the passage of cold fronts.

The effect of the Madden-Julian Oscillation (MJO) on SAMS onset was also analyzed. The WR and the SACZ did not show a clustering of onset dates within the enhanced phases of the MJO for South America, therefore onset in those regions is found to not be affected by the MJO.

ROLE OF COLD FRONTS IN SOUTH AMERICAN MONSOON ONSET

A Thesis

Presented To

the Faculty of the Department of Geography

East Carolina University

In Partial Fulfillment

of the Requirements for the Degree

Masters of Arts

by

Emily A. Wright

July 23rd, 2010

ROLE OF COLD FRONTS IN SOUTH AMERICAN MONSOON ONSET

by

Emily A. Wright

APPROVED BY:

DIRECTOR OF

DISSERTATION/THESIS:_____Dr. Rosana Nieto-Ferreira, PhD.

COMMITTEE MEMBER: _____Dr. Tom Rickenbach, PhD.

COMMITTEE MEMBER: _____Dr. Scott Curtis, PhD.

CHAIR OF THE DEPARTMENT OF

GEOGRAPHY:_____Dr. Burrell Montz, PhD.

DEAN OF THE GRADUATE

SCHOOL:_____Paul J. Gemperline, PhD

ACKNOWLEDGEMENTS:

I would like to thank my advisor and my committee for their dedication, guidance, and patience throughout the writing of the thesis.

I would like to thank my outside reader, Dr. Sid Mitra, for his input during the thesis process.

I would also like to thank Richard Barnhill for his support and contribution to the thesis.

I would like to thank my parents for providing this opportunity to attend East Carolina University, and for their love and encouragement through this process.

TABLE OF CONTENTS

LIST OF TABLES:

LIST OF FIGURES

1. INTRODUCTION:

The South American Monsoon System (SAMS) is an integral part of the lives of people in South America. Countries such as Brazil depend on rainfall for sugar cane production and hydroelectric power as a major source for energy and fuel (Rickenbach et al. 2009). The variability of the monsoon onset is important to the agriculture and energy sectors of Brazil (Grimm and Zilli, 2009). In addition to the monsoon, cold fronts bring rainfall to the region year-round. Cold fronts that occur east of the Andes Mountains are an important mode of synoptic-scale variability in South America (Garreaud and Wallace, 1998; Garreaud, 2000). However, there has been little work on the impact cold fronts have on the onset of SAMS.

1a. Monsoons

The broad definition of a monsoon is the seasonal reversal in the large-scale circulation driven by the differential heating of the continents and the oceans (Zhou, 1998). There are criteria for determining if a region experienced a monsoon season. Ramage's (1971) revised criteria based on Khromov's (1957) monsoon definition became the standard for selecting monsoon regions (Zhou, 1998). Ramage (1971) stated that a monsoon region requires a prevailing wind direction shift of at least 120° between January and July, the average frequency of prevailing wind directions, or the wind direction with the highest percent of frequency in a given area, is greater than 40 % of total wind directions during January and July, the mean wind in at least one of the months is greater than 3 m/s, and that circulation fluctuates between a cyclone and anticyclone less than one time every two years in either January or July in a 5° latitude-longitude rectangle. Therefore, the only region that satisfied all requirements was a region extending from 20°W to 170°E, and 35°N to 30°S (Ramage, 1971). This region includes the well documented east Asian summer monsoon (EASM; Zhou, 1998). Therefore, according to

his criteria, Ramage (1971) states that South America is monsoonless because there is no seasonal reversal of lower level wind direction, which can be attributed to two reasons. One reason is the geography of the continent, specifically the narrow part of the continent furthest away from the equator which could limit the formation of stationary highs and lows- one of the requirements of a monsoon region according to Ramage (1971). Second, Ramage (1971) states that the constant upwelling of ocean water along the west coast of South America keeps the sea surface temperatures (SSTs) lower than surface air temperatures of the continent throughout the entire year. Until recently, Ramage's (1971) argument for a monsoonless South America has prevailed. Zhou and Lau (1998) argue there is a monsoon in South America, based on similar circulation characteristics between the EASM and the South American Monsoon System (SAMS). For example, Figure 1 shows a comparison of circulation features between the EASM and the SAMS taken from Zhou and Lau (1998). Upper and lower tropospheric circulation features highlighted by the map show similarities between the EASM and SAMS, including the Gran Chaco low in South America and the EASM trough, the South Atlantic Convergence Zone (SACZ) off the coast of Brazil and the Mei-Yu front zone in China, and the upper-tropospheric Bolivian high and the Tibetan high. The similarities between the SAMS and the EASM led Zhou and Lau (1998) to conclude there is a monsoon region in South America.

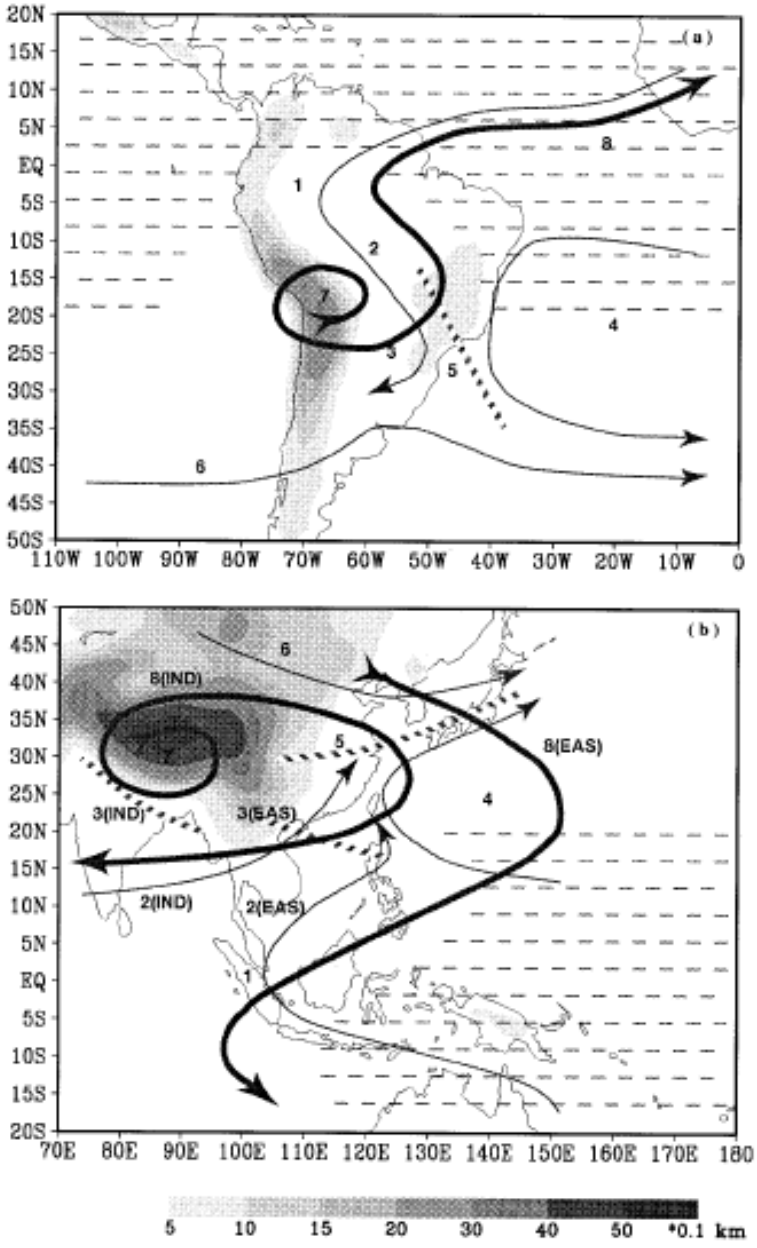

Figure 1: Circulation features of the SAMS and the EAS. The features are numbered accordingly and are as follows: 1) low-level cross equatorial flow, 2) South American Low-Level Jet and southwesterly flow over Southeast Asia, 3)Gran Chaco low and EASM trough, 4) subtropical high, 5) SACZ vs. Mei-Yu front zone, 6) midlatitude westerlies, 7) Bolivian High and Tibetan High, and 8)upper-level return flow. From Zhou and Lau (1998).

In addition to the circulation features, South America's monsoon is characterized by a dry phase during the winter and a wet phase during the summer (Zhou and Lau, 1998). The onset of the wet phase of the monsoon is characterized by a change of circulation with the establishment

of the upper level Bolivian High. The Bolivian High, formed by increases in latent heat flux of convection, diverts upper-level circulation to curve around the Bolivian High as it strengthens during the summer months (Lenters and Cook, 1997). This curvature of the westerlies can lead to rapid strengthening of disturbances and differences of orientation and speed of these disturbances (Lenters and Cook, 1997). In addition, the Nordeste Low is an upper level trough that is centered off the coast of Northeast Brazil. It feeds off cold air from the polar region and reaches its maximum in the southern hemisphere summer months (Lenters and Cook, 1997). Convection shifts from northwestern South America to central Amazonia and central Brazil. Typically during monsoon onset, the sea level pressure in the South Atlantic falls and the South Atlantic Subtropical High shifts eastward and weakens. This change contributes to the general decrease in sea-level pressure in the Southeastern part of South America. With the decrease in sea-level pressure, the winds shift from easterlies to northeasterlies. All of these conditions result in the southward displacement of convection and an increase in precipitation, in an area that extends from the Amazon to southeastern Brazil (Raia and Cavalcanti 2008).

There is a significant change in upper-level circulation between the winter and summer season in South America. According to Kruels, et al. (1975) and Silva Dias, et al. (1983), during the winter there are strong mid-latitude westerlies at 200 mb. Atmospheric systems that move into into South America from the Pacific Ocean tend to follow these westerlies. Figure 2 shows the climatological atmospheric circulation for both winter and summer in South America. Figure 2 illustrates rainfall patterns and 200 mb and 700 mb streamlines for the winter and summer season. The 200 mb (Figure 2e) streamline plot for the summer season displays the westerlies in the mid-latitudes of South America. The plot shows an established anticyclone (the Bolivian

High) over the Amazon that disrupts the mid-latitude westerly flow, causing disturbances to curve northward around the High (Kruels et al., 1975 and Silva Dias et al., 1983).

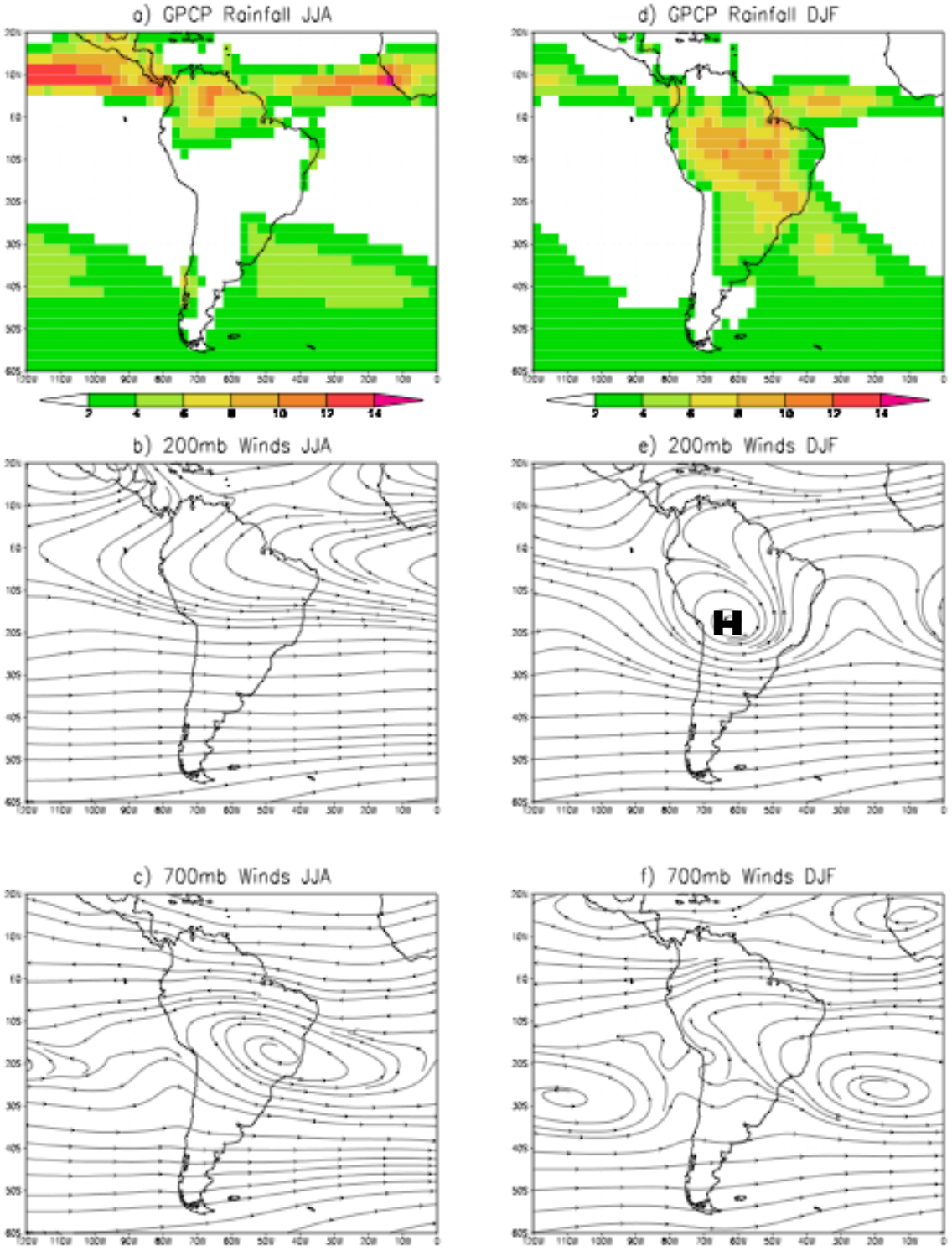

Figure 2: GPCP rainfall (mm/day), 200 mb streamline), and 700 mb streamline (based on NCEP/NCAR data) patterns for winter (JJA) and summer (DJF)

The South America monsoon onset has been previously defined using Outgoing Longwave Radiation (OLR), rainfall, and low-level meridional winds. A threshold for onset in terms of OLR, which indicates high cloudiness likely associated with convection and rainfall, was defined by Kousky (1988) as the time when OLR falls below 240 Wm^{-2} with 10 of the previous 12 pentads having OLR greater than 240 Wm^{-2}. The end of the wet season sees just the opposite. However, using OLR for determining onset has disadvantages. OLR only provides a very rough estimate of rainfall amounts and therefore OLR thresholds can only determine the approximate onset and end dates of the wet season. These disadvantages have led other studies to use rainfall data to determine the beginning and end of the monsoon season. For instance, Marengo (2001) defined the monsoon onset date as the pentad that has greater than 4 mm/day daily average precipitation with 6 of the previous 8 pentads having less than 3.5 mm of average rainfall per day and 6 of the 8 following pentads having greater than 4.5 mm/day daily average precipitation (Marengo 2001). Raia and Cavalcanti (2008) base their definition of onset on a vertically integrated moisture flux. As the wind changes from northerlies to northwesterlies over southwestern Amazon and from easterlies to northeasterlies in eastern Brazil, they contribute to the increased moisture flux into the monsoon region (Raia and Cavalcanti, 2008). As onset begins, the moisture flux intensifies and continues to draw moisture into the monsoon area. Therefore they determined that an intensification of the moisture flux into the monsoon region was essential for onset to occur (Raia and Cavalcanti, 2008).

What makes the SAMS unique is the timing of the monsoon onset. During the months of September- October, onset is characterized by a slow change from dry to wet season brought on by the migration of the sun and the Intertropical Convergence Zone (ITCZ) (Horel, 1989) in the northwest and west portions of Brazil. By November, the onset of the monsoon becomes rapid as

it spreads southeastward. This rapid onset may stem from the development of cold fronts and the SACZ in the area at the time of onset (Nieto Ferreira and Rickenbach, 2010, hereafter NR10). Both features will be discussed in detail later.

Li and Fu (2006) set the backdrop for this study. The region that Li and Fu (2006) used to determine onset is a large area that spans from western Amazon to southeast Brazil. By encompassing this large of an area, they assume that onset is regionally uniform. However, it was demonstrated by previous studies (e.g., Marengo et al 2001, NR10) that monsoon onset varies from region to region. Therefore, this study will focus more on the regional variability of onset. Li and Fu (2006) use the European Centre for Medium-Range Weather Forecasts Re-Analysis (ERA) rain data to determine monsoon onset. However, the ERA rainfall data is a model product, not data, and does not well represent the precipitation patterns of rain observed by rain gauges or by the Global Precipitation Climatology Project (GPCP). Thus this study will use GPCP data, which is a combination of rain gauges and observations, and will better represent the precipitation patterns across South America. Although Li and Fu (2006) examine the role of cold fronts on monsoon onset, they did not incorporate the regional variability of onset. This variability of onset may be a product of cold fronts passing through the area.

1b. Cold Fronts:

Cold fronts that flow across South America may have an impact on the onset of the South American Monsoon System (SAMS). Cold fronts typically are centered to the east of the Andes Mountains. With a period of one to two weeks, cold fronts occur year round (Garreaud, 2000). Garreaud (2000) analyzed sea-level pressure (SLP) tendencies and selected days that had SLP tendencies at the top 10% of the seasonal frequency distribution. These episodes were labeled

cold surges, or strong cold fronts. Garreaud (2000) indicated that a cold surge was defined as having a 1.5 mb increase in SLP over 24 hours, only retaining episodes that were above 1015 mb (1020) for the summer (winter).

According to Garreaud (2000), cold surges that occur during the cold season tend to have more dramatic fluctuations in temperature and pressure, with some of the more extreme fluctuations resulting in sub-freezing temperatures in areas that would typically experience a temperate cold season. Cold surges that occur during the warm season have weaker temperature fluctuations, but tend to have more precipitation associated with the cold surges. Figure 2 shows the map composites of the Convective Index (CI) and CI anomalies based on OLR for both the wintertime and summertime seasons. CI can interpret convection based on cloudiness from OLR data and it increases with colder cloudiness. Day 0 represents the mature stage of the cold surge. For the wintertime season, Garreaud (2000) observed that there was no CI signature apparent in South America. As the cold surge approached the study area (25°S, 57.5°W) on Day -1 (Figure 2a), there was a small area of CI and CI anomalies (shaded) off the coast of southeast Brazil, but it quickly weakened as the cold surge passed through the study area on Day 0 (Figure 2b) and Day +1 (Figure 2c) (Garreaud, 2000). The summertime composite map shows a different scenario. There is an area of increased CI over the Amazon Basin as the cold surge passes through on Day 0 (Figure 3e), which migrates northwestward as the cold front exits Garreaud's (2000) 25°S, 57.5°W study area. Therefore, the presence of CI values in the summertime suggests that cold surges bring enhanced convection to central and south east Amazon, whereas the lack of CI values in the wintertime suggests the wintertime cold surges do not (Garreaud, 2000).

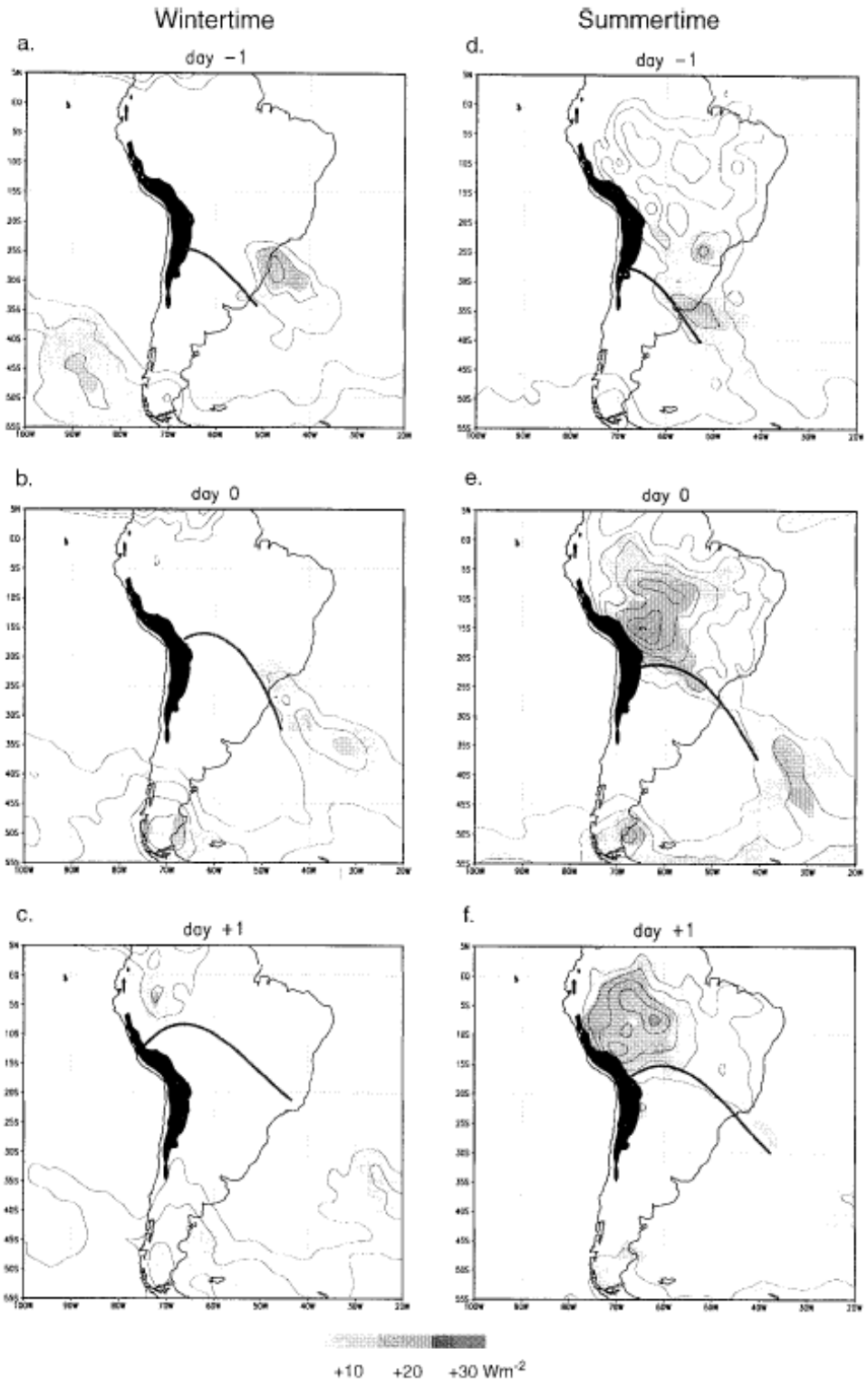

Figure 3: Composite maps of Convective Index (CI; contoured every 10W/m^{-2}) and CI anomalies (shaded) during wintertime and summertime. Day 0 indicates mature stage of cold surge. Black line indicates location of cold surge. From Garreaud (2000).

Cold fronts are bounded and shaped by the presence of the Andes Mountains. The Andes Mountains, located in the western part of South America, extend north-south from roughly 10˚N to 50˚S. The highest peaks tend to be located at 30˚S, which act as a barrier for atmospheric low-level airflow travelling west to east. Since airflow is not blocked south of 40˚S, the disruption of flow north of 40˚S causes the increase of the anticyclonic curvature of the migratory systems. The increased curvature of the migratory systems pull cold air northward over South America. This pattern of northward deflection occurs in all seasons; however it is strongest during the winter season when the baroclinic regions are displaced to regions of higher orography (Seluchi 1998).

Other studies have looked at cold fronts and how they might be influenced by the Andes Mountains. According to Lupo et al. (2001), South American cold fronts are marked by a strong ridge over western South America and a deep trough over the Atlantic. This assists the channeling of cold air towards the equator. It has been stressed that this pattern stems from the effect the Andes has on the cold fronts. Lupo et al. (2001) classified cold fronts into three types based on intensity of the cold surges through a measurement of 1000-850 hPa thickness of mean temperature.

Raia and Cavalcanti (2008) also analyze cold fronts in their study of the South American monsoon onset. Cold fronts contribute rainfall as well as modify the humidity, and fluxes of heat and momentum to mainly the subtropical and middle latitudes. In order to determine the role of cold fronts in monsoon onset, Raia and Cavalcanti (2008) looked at three years: 1998 (normal onset), 1991 (late onset), and 2001 (early onset). They averaged SLP, precipitation, temperature, specific humidity, latent and sensible heat flux, soil moisture, and several other atmospheric variables over the area bounded by 17.5°-22.5° S, 42.5°-47.5° W. In general, several cold fronts

pass through the study region before onset, sometimes associated with rainfall. The fronts increased soil moisture and latent heat flux, as well as added to the northwesterly flow increase east of the Andes due to the pressure decrease as the cold fronts approached southeast Brazil (Raia and Cavalcanti, 2008). The convective instability from the cold fronts present favorable conditions for onset to occur.

During the normal onset of the Raia and Cavalcanti (2008) study, not only are cold fronts evident before onset, but humidity, soil moisture, and latent heat flux all increase gradually, and sensible heat flux decreases. In the late onset, the SLP average in southeast Brazil from August to middle September is greater than in the normal onset, and there was no precipitation associated with the passage of cold fronts in August or September. However, as soon as the SLP began to decrease, there was precipitation associated with the cold fronts. Raia and Cavalcanti (2008) noticed two false onset episodes that occurred within the late onset scenario, where atmospheric conditions such as sustained precipitation and an increase in humidity developed, but soon diminished, resulting in a late onset. As soon as a cold front passed through, bringing sustained precipitation and elevated humidity levels, the area reached the necessary conditions for onset to occur. The third scenario, early onset, saw higher than usual SLP values during August, but SLP decreased sharply with the passage of a strong cold front that brought the necessary atmospheric conditions for onset to occur. Raia and Cavalcanti (2008) also suggest that cold fronts moisten the soil and the troposphere from western Amazon to southeast Brazil due to increased levels of relative humidity and rainfall.

Li and Fu (2006) analyzed cold fronts from 1979-1993. Using only the strongest 10% of cold fronts that have pressure values greater than 1018 mb during October to November, they concluded that cold fronts occurred either a pentad, or a five day average, before onset or within

the same pentad of onset within their defined region called Southern Amazon, or an area bounded by 5°–15°S, 45°–75°W. Therefore, cold fronts can assist in changing the thermodynamic structure and circulation of the atmosphere, and thus can trigger the monsoon onset. Li and Fu (2006) concluded that analyzing the thermodynamic conditions of the atmosphere would lead to determining the cold front event that would trigger the monsoon onset.

However, previous studies have been uncertain on how cold fronts affect the monsoon onset since there are many features that are present during the SH summertime months. Another factor of summertime convection is the establishment of the South Atlantic Convergence Zone (SACZ).

1c. The South Atlantic Convergence Zone (SACZ)

The SACZ is a band of cloudiness that extends from the Amazon Basin into the South Atlantic Ocean (Liebmann et al., 1999), and is the most distinguishable in the summertime months (DJF). The SACZ and the convective activity in the Amazon basin are the main components of SAMS (Carvalho et al., 2004). There are more prominent intraseasonal variations in convection over eastern South America than found in the Amazon Basin (Liebmann et al., 1999). Since the SACZ can occasionally extend into the Amazon, Carvalho (et al.,2004) labeled three regions within the SACZ- the Amazon, Coastal, and Oceanic regions. These regions represented the regions with the maximum convective activity. The Amazon region showed the minimum subseasonal variance, and the coastal and oceanic regions showed maximum subseasonal variance (Carvalho et al., 2004). The SACZ can exhibit changes in its geographic extension; in some cases the SACZ can extend from the Amazon to the Atlantic Ocean, or just cover portions of Brazil (Carvalho et al., 2004). Cold fronts can contribute to the convective activity in the SACZ region, especially during the summertime. Garreaud and

Wallace (1998) concluded that the cold fronts are the dominant pattern of the daily variability of deep convection, and can contribute about 25% to summertime precipitation in the central Amazonia and about 50% of precipitation over the subtropical plains of South America. This was confirmed by Liebmann et al. (1999)

1d. The Madden-Julian Oscillation (MJO)

The Madden-Julian Oscillation (MJO) is an eastward propagating mode of tropical interseasonal variability that has a period of 30-60 days and affects monsoons all over the globe (Madden and Julian, 1971; Nogues-Paegle et al., 1997; Jones and Carvalho, 2002; Jones and Carvalho, 2006). The MJO is controlled by the latitudinal position of the tropical heat sources and can affect rainfall and extreme events in many areas (Jones and Carvalho, 2006). The MJO can be characterized into eight different phases depending on the longitudinal position of the rainfall associated with it. Each phase of the MJO has a distinct signature in atmospheric variables (Wheeler and Hendon, 2004). Wheeler and Hendon (2004) defined eight phases for the MJO based on a combined Empirical Orthogonal Function (EOF) analysis of OLR, 850 hPa zonal wind and 200 hPa zonal wind. Figure 4 shows rainfall for the eight phases of the MJO cycle during November-March. Areas in green represent enhanced convection, and brown areas represent suppressed convection. For example, in Phase 1 (Figure 4), enhanced convection is present in the West Indian Ocean. Phases 7 and 8 in Figure 4 show significant enhanced convection for southeastern Brazil, whereas Phases 3 and 4 show suppressed convection for SE Brazil.

Previous studies have suggested that the MJO is linked to SAMS rainfall variability, but there is no clear connection between MJO and SAMS onset. Raia and Calvacanti (2008) did find that a blocking pattern of upper-level winds for a frequency characteristic of the MJO occurs

when the SAMS onset is later than normal. Carvalho et al. (2004) also found an increase in extreme rainfall events for the SACZ during December-February when the MJO suppressed convection over Indonesia and enhanced convection in the central Pacific. This is in good agreement with Figure 4 which shows enhanced convection over South America during times when there is enhanced convection in the central Pacific; (Phases 7 and 8) (Carvalho et al. 2004).

Other monsoon regions throughout the globe are affected by the MJO. Wheeler and Hendon (2004) concluded that both the Indian and Australian monsoon onsets tend to occur during their respective local convectively enhanced half of the MJO cycle (i.e. four out of eight phases of the cycle where there are areas of enhanced convection near the monsoon regions) and rarely occur within the local suppressed half of the MJO cycle.

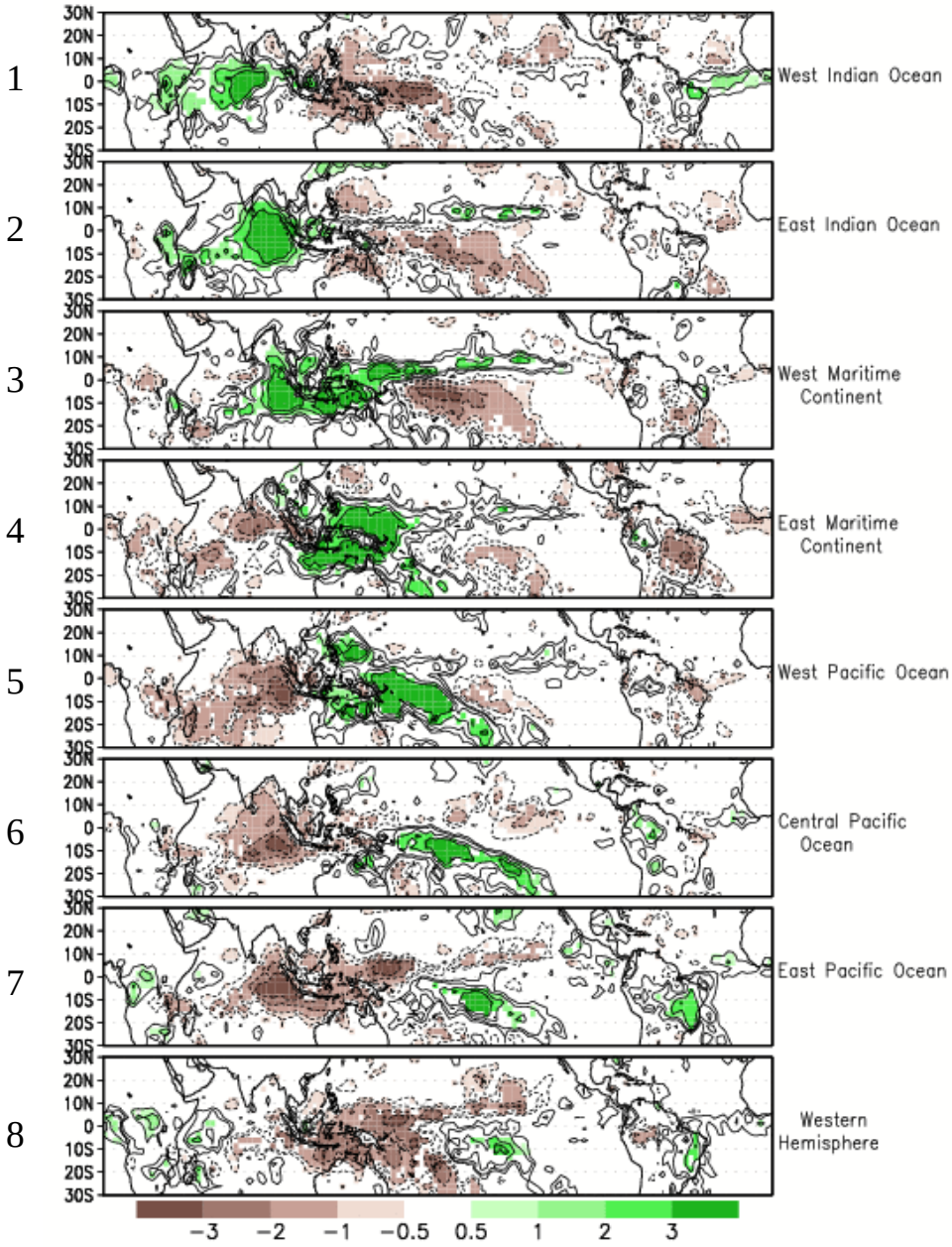

Figure 4: Composites of rainfall for the eight phases of the MJO cycle during the period of November through March. Rainfall anomalies are contoured and areas of statistical significance (at the 95% level) are shaded. Units are in mm/day. (From the Climate Prediction Center website, adapted from Wheeler and Hendon,2004)

2. RESEARCH QUESTIONS:

The objective of this study will be to understand how cold fronts impact onset of the South American Monsoon System. The dates of onset of the South American Monsoon vary from year to year, and also from one South American region to another. In fact, monsoon onset does not happen at once for all of South America, instead it gradually spreads into the continent with different regions of South America having different monsoon onset dates (NR10 and Marengo, 2001). NR10 analyzed regional variability for monsoon onset and proposed a three-stage conceptual model. They concluded that the first stage of onset started in mid October in the northwestern portion of South America and was due to the slow thermodynamic changes associated with the gradual migration of the sun into the Southern Hemisphere. The second stage is marked by the abrupt establishment of the South Atlantic convergence zone around late October. The third stage is monsoon onset near the mouth of the Amazon River in late December due to the Atlantic Intertropical Convergence Zone that moves into the area (NR10). The three-stage model therefore demonstrates the variability of onset in tropical and subtropical South America. Some of this interannual and spatial variability could be attributed to cold fronts.

This study has two main objectives. First we will focus on the timing and structural changes of the cold fronts to determine whether there are significant associations between cold fronts and SAMS onset. Next, if we find in the first part of the study that cold fronts indeed affect the onset of the monsoon season, we will clarify in what regions of South America monsoon onset is affected by cold fronts and if there are any remote influences on onset, such as the Madden-Julian Oscillation (MJO).

3. METHODOLOGY:

This study includes an analysis of cold fronts during the South American Monsoon onset. Data will be analyzed based on a selected study area within South America.

3a. Study area:

The study area will consist of four regions listed on the map (Figure 6) that correspond to areas of distinct variability of the annual cycle of rain, as determined by the rotated Empirical Orthogonal Function (REOF) analyses done by NR10 of the GPCP rainfall pentads. A REOF analysis deconstructs the GPCP rainfall data and can find both time and spatial patterns within the data. Therefore, the REOF analysis is suited to capturing rainfall variability within regions of South America (NR10).

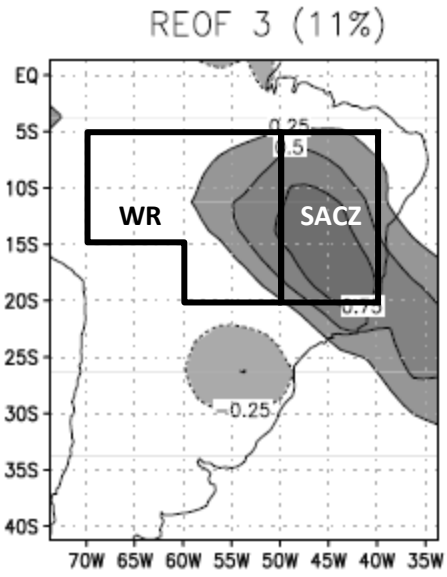

Figure 5: Third REOF from 1979 to 2007. Boxes show West Region and SACZ region. Adapted from NR10.

The regions are listed as the West Region (WR), The East Region (ER), the South Atlantic Convergence Zone Region (SACZ), and the South Region (SR). Figure 5 shows the third REOF mode. The third mode of the REOF analysis (Figure 5) shows

strong signatures of rainfall variability in the SACZ region (NR10). In addition, REOF1 (not shown) captures the annual variability of convection in the Amazon Basin and is used in a similar fashion to the SACZ to determine onset in the Amazon Basin. These two modes correspond to the regions defined as the WR and the SACZ. These regions are the basis for the regional study using daily National Center for Atmospheric Research and the National Centers for Environmental Prediction (NCAR/NCEP) reanalysis data. This study focuses on the SACZ and WR. Rainfall in the SACZ region can be attributed mainly to frontal systems that pass through the area (Garreaud and Wallace, 1998). The WR is centered on the Amazon Basin and is an area of intense convective activity. The WR is also used for comparison to the SACZ region because both areas see similar convective activity, but experience different timings of onset- WR has a more gradual onset due to the movement of the sun, and the SACZ has a more abrupt onset associated with the establishment of the SACZ. A more thorough analysis of the ER and SR is found in Barnhill et al. (2010).

3b. Data:

For this study NCEP/NCAR (Kalnay et al. 1996) data will be used. This data is constructed from assimilation into a global atmospheric model to produce globally uniform wind and thermodynamic fields (Kalnay et al. 1996). Data are provided at 17 pressure levels from 1000 mb to 10 mb (Kalnay et al., 1996) and 2.5° horizontal resolution. For this study, the sea-level pressure, 925 mb temperature, 925 mb wind vectors, 925 mb specific humidity, 200 mb winds, 200 hPa geopotential height, and latent and sensible heat fluxes will be used. The height levels are chosen to analysis both the upper and lower levels of the atmosphere. The heat fluxes are chosen to understand thermodynamic changes in the atmosphere. The range of data used for

this study will be from January 1, 1998 to December 31, 2008 in order to be in agreement with the GPCP rainfall data (Kalnay et al., 1996).

Figure 6: Map showing numbered 5° by 5° boxes with study regions outlined in black. Adapted from NR10.

In addition to the NCEP/NCAR Reanalysis Data, this study will include the GPCP data, which is a combination of satellite data and rain gauges (Huffman et al., 2001). The GPCP Data is available from 1997 to the present at a 1° resolution. This data will be used to construct the composites of cold fronts during monsoon onset discussed later.

For further investigation of the WR and the SACZ, onset pentads for each year were again determined using a REOF analysis of the GPCP rainfall pentads. The third mode of the REOF analysis (Figure 7) shows strong signatures of rainfall variability in the SACZ region. For each year, SACZ onset was defined as the time when the principal component timeseries (Figure 7) for REOF3 becomes negative and stays negative for at least six of the next eight pentads.

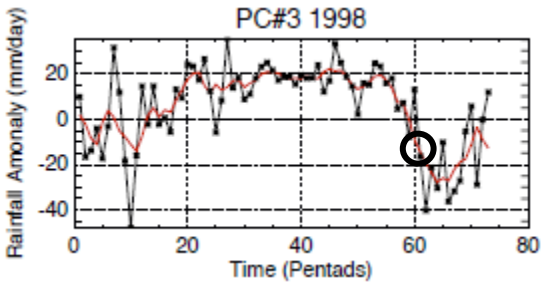

Figure 7: REOF3 timeseries for 1998 with onset pentad marked with an 'O'.

In the SACZ region convection is influenced from the passing of the cold fronts during the summertime (NR10). The onset pentad dates for the SACZ region calculated for 1998-2008 are listed in Table 1. These onset dates will be used to calculate "pre-onset" and "post-onset" cold fronts composites to determine the role of cold fronts on monsoon onset in different regions of the SAMS. The average onset pentad for the SACZ region is pentad 62 (2 November- 6 November).

Year	1998	1999	2000	2001	2002	2003	2004	2005	2006	2007	2008
Onset Pentad	61	59	61	57	69	62	64	61	58	66	63
Onset Dates	28 Oct-1 Nov	18-22 Oct	28 Oct-1 Nov	8-12 Oct	7-11 Dec	2-6 Nov	13-17 Nov	28 Oct-1 Nov	13 - 17 Oct	22 - 26 Dec	8 – 12 Nov

Table 1: REOF onset pentads from 1998-2007 for the SACZ region (From NR10).

A compilation of cold fronts that have occurred during 1998-2008 was also produced by NR10. The dates of cold fronts were determined based on a slightly modified version of the Garreaud (2000) definition of cold surges. The decrease in sea-level pressure, according to the definition, was determined in a 5° by 5° grid box centered at 25°S, 57.5°W (Garreaud, 2000). However, definitions of a cold surge according to Garreaud (2000) restricted the data to only one or two very strong cold fronts per month in November-December. In this study the Garreaud (2000) cold surge criteria was relaxed to include all cold fronts that passed through South America during August through December. In the present study, initially a cold front is defined - when a 1.5 mb decrease in sea-level pressure occurs over a period of one day, for sea-level pressure greater than 1010 mb. To make sure that a single cold front episode was not repeated when averaged, cold fronts that persisted for several days were only counted once. A climatology for the years 1979-2008 was constructed to understand how the frequency of cold fronts changes for each month for the 1010 mb threshold. To determine whether the majority of the cold fronts were captured within the 1010 mb threshold, the sea-level pressure was dropped to a 1005 mb threshold to allow for comparison between the two thresholds.

3c. Analysis:

Given the structure of the SACZ and the abruptness of its onset, cold front composites for the 11 years from 1998-2008 were focused around the date of onset for the SACZ region. Three scenarios were analyzed: a "pre-onset" cold front composite for the last cold front that occurred before the onset pentad of each year; an "onset" cold front composite, or the cold front that occurred during the onset pentad; and a "post-onset" cold front composite, or the first cold front that occurred after the onset pentad. All cold fronts from 1998-2008 that occurred during those three scenarios were averaged for each composite. Rainfall, upper-level geopotential height

anomalies, lower level wind anomalies, sea-level pressure anomalies, and lower level temperature anomalies were plotted to study any differences between "pre-onset", "onset" and "post-onset" cold fronts. Anomalies were derived based on the 1998-2008 climatological mean. In the "pre-onset" plots, Day 0 represents the last cold front to occur before monsoon onset. In the "onset" plots, Day 0 represents the cold front that occurred during the onset pentad, and the "post-onset" plots show Day 0 as the first cold front to occur after the monsoon onset. Days -3, -2, -1 represent three, two, and one day before the cold front passed through the 5° by 5° grid box centered at 25°S, 57.5°W box. Days +1 and +2 are one and two days after the cold front. This analysis is similar to studies done by Garreaud (2000) and Li and Fu (2006).

To elucidate the regional differences in monsoon onset, pentad averages of NCEP/NCAR reanalysis variables in each region were analyzed for the years 1998-2007. This analysis included NCEP/NCAR reanalysis sea-level pressure, potential temperature, and latent and sensible heat flux. The data were averaged over the ten-year span and plotted as pentads. The pentads were averaged again over each of the four regions (SACZ, WR, SR, and ER). The regions allow for comparison between different areas within South America not done in previous studies.

In addition, SACZ region case studies were analyzed for the years that had an early or late onset. 2006 was a year with an early onset in the SACZ region, and 2007 had a late onset in the region. Similar to the NCEP/NCAR regional analysis, sea-level pressure, potential temperature, specific humidity and latent and sensible heat flux were used to establish differences in the atmosphere for an early or late onset. This analysis follows the early/late onset comparison of Li and Fu (2006) in order to better understand the atmospheric conditions present

that precede an early and late onset. The early/late onset comparison analysis will also reveal whether cold fronts play a large role in triggering monsoon onset.

Lastly, we analyze a possible role of the MJO in SAMS onset. The MJO index used was Real-Time Multivariate MJO series (RMM1 and RMM2), created by Wheeler and Hendon (2004). This index is based on a combined EOF analysis of averaged OLR, 850-hPa zonal wind and 200-hPa zonal wind with longer timescales removed. The RMMs represent the two principal components from the combined EOF analysis (Wheeler and Hendon, 2004). Wheeler and Hendon (2004) compared the Indian and Australian monsoon onsets to the RMM1 and RMM2 index. This index already has demonstrated that the Indian and Australian monsoon onsets tend to occur during the convectively enhanced half of the MJO cycle, and rarely within the suppressed half of the MJO cycle (Wheeler and Hendon, 2004). Carvalho et al. (2004) suggested that extreme rainfall events increased within the SACZ region when the MJO phases had enhanced convection in the central Pacific and over the SACZ region. Based on these criteria, MJO phases 7 and 8 (Figure 4) were chosen as showing enhanced convection in the central Pacific and near the SACZ. Pentad averaged RMM1 and RMM2 values for SACZ and WR onset for each year were calculated and plotted as an MJO phase diagram. Only onset years that fell into the "significant" area of the cycle, or outside the inner circle of the phase diagram, were analyzed. This diagram was used to see if SACZ and WR onset occurred during times when the MJO acted to enhance convection over the SACZ and the WR, namely phases 7 and 8 of the MJO cycle.

4. RESULTS:

For each August-December month from 1998-2008, composites of cold front structure in terms of their averaged GPCP rain, low-level temperature, sea-level pressure, 925 mb winds, 200 mb geopotential height, and 200 mb streamfunction have been calculated. Figure 8 shows the averages of all cold front events for each month of the example year (2004). 2004 was chosen as it depicted an accurate view of what most of the cold fronts looked like from 1998-2008. GPCP rainfall is plotted as well as 200 mb streamfunction, both averaged by month. Figure 8 is an example of the typical seasonal variability of the structure of cold fronts in South America.

The onset in the WR in 2004 occurs at pentad 58 (October 13^{th}-17^{th}). This onset is clearly shown during the month of October in Figure 8 by the increased precipitation area in western Amazonia. In October, the convection has just started to reach the SACZ region. In the months of November and December, there is precipitation that extends from western Amazonia to southeastern Brazil. This increased precipitation shows that the average cold front has an increased amount of precipitation associated with it that is being brought to the SACZ region than in September. The reappearance of the precipitation in the SACZ region in November and December displays that onset has occurred in the SACZ region.

During the month of August, the 200 mb streamfunction shows upper level circulation that resembles wintertime circulations presented by Horel et al. (1989) and Silva Dias et al. (1983) By October, the Bolivian High has already been established in Amazonia,. Since the Bolivian High forms due to latent heat released by convection in the Amazon, the anticyclone found in the 200 mb streamfunction composites confirms that onset has occurred in the WR during October.

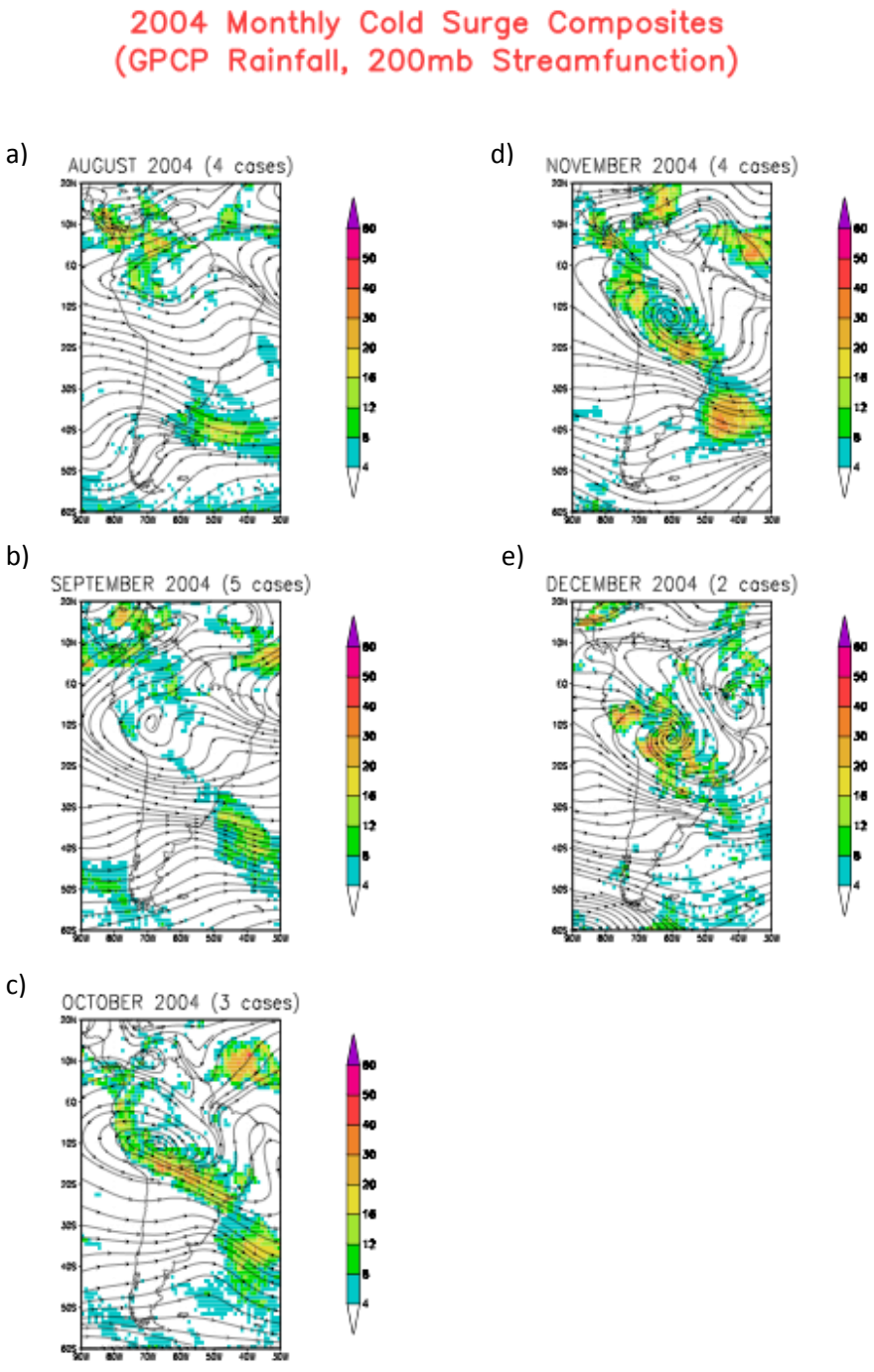

Figure 8: Monthly Cold front Composites for August-December with GPCP rainfall (shaded) and 200 mb streamfunction (contoured).

4a. Frequency of Cold fronts

Figure 9 shows the average number of cold fronts by month found using a threshold of 1010 mb during 1979-2008. The average number of cold fronts is highest in the winter months, with a peak in the month of July. During spring and into the summer months, the number of cold fronts drops off sharply and is less than 5 cold fronts for the summer months. This result is similar to seasonal cold front studies done by Lupo et al. (2001). They found the largest number of cold fronts to be within the winter months with a maximum in July. Garreaud (2000) states that the anticyclones associated with wintertime cold fronts have higher SLP than the summertime cold fronts. To make sure all cold fronts, especially ones in the summertime months, were accounted for, the SLP threshold was dropped to 1005 mb. The new definition of a cold front is a 1.5 mb increase in SLP over 24 hours for values greater than 1005 mb. Figure 8 shows the histogram of cold fronts that meet these requirements.

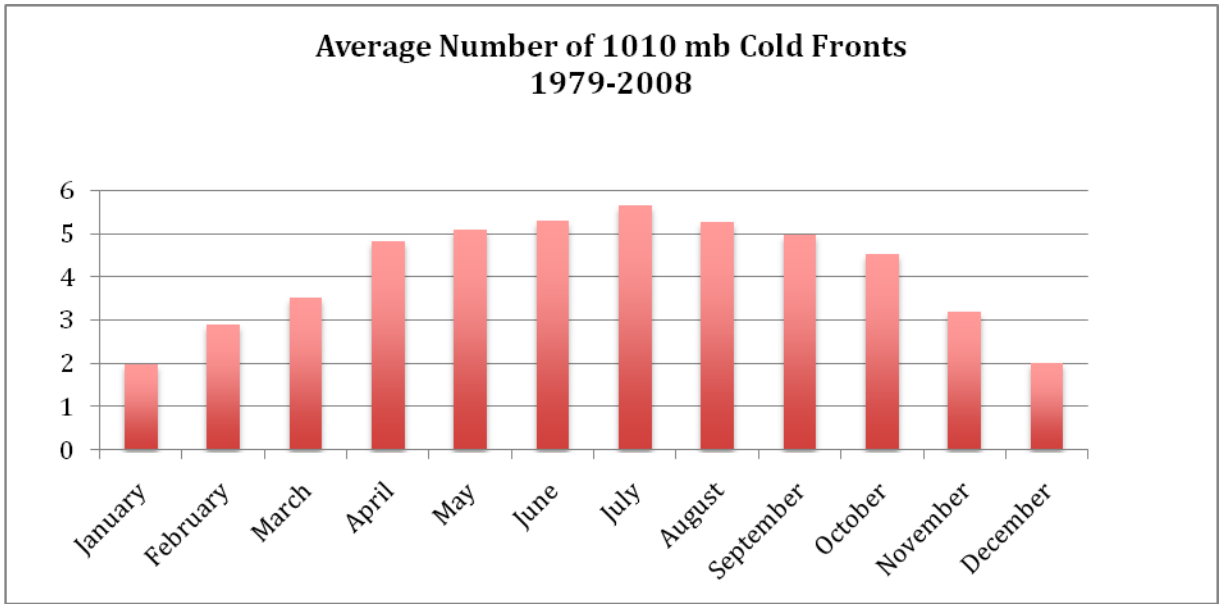

Figure 9: Average Number of Cold fronts by Month for 1010mb based on SLP (in mb) from NCEP/NCAR reanalysis

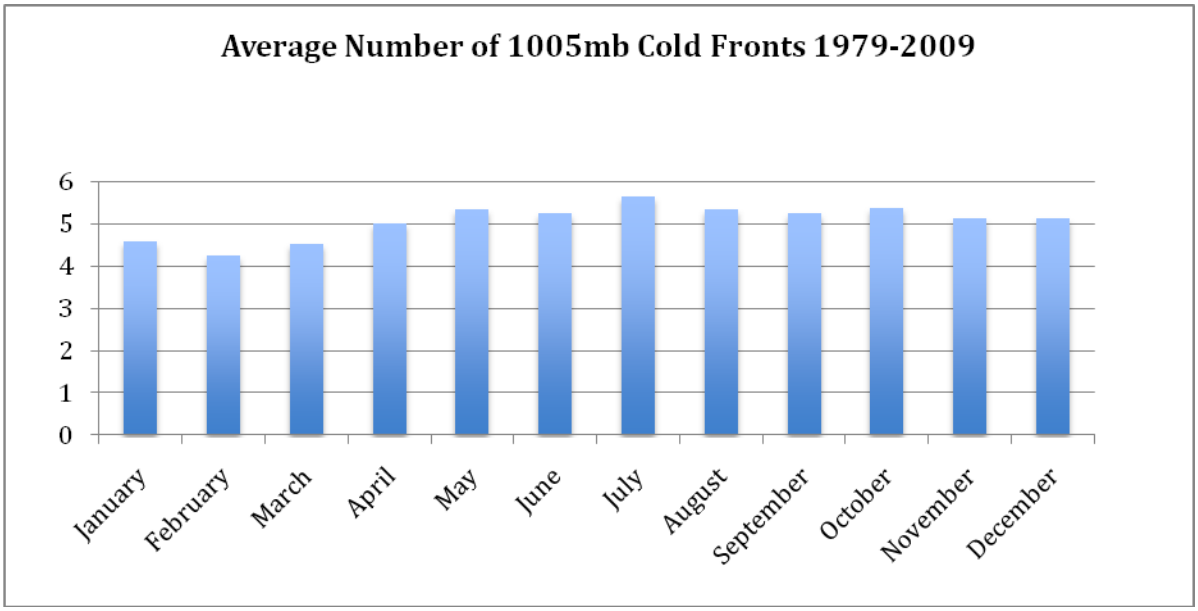

Figure 10: Average Number of Cold fronts by Month for 1005mb based on SLP (in mb) from NCEP/NCAR reanalysis

For Figure 10, dropping the SLP threshold to 1005 mb increases the number of cold fronts found in the summertime months. July is still the month that has the greatest amount of average cold fronts.

4b. Regional Onset Analysis

Pentad timeseries averages were analyzed for the years 1998-2007. Variables from the NCAR/NCEP reanalysis data were chosen, including sea-level pressure, potential temperature, and latent and sensible heat flux. The data are averaged by pentads over ten years to show the seasonal cycle for each variable. The pentads were averaged again over the four regions shown in Figure 6.

In Figure 11a, the WR and ER show an increase in sea-level pressure during the winter pentads, and a decrease into the summer pentads. This increase in the winter and decrease in

summer of the SLP shows that the annual cycle is present in the WR and ER, as well as the SACZ region and the SR. The SACZ region shows a similar pattern to the WR and ER, however the SACZ region has a higher overall SLP than the WR and the ER. This is due to the SACZ region's relatively closer location to the South Atlantic Subtropical High (Fig11a). The SR shows the highest SLP of all the four regions.

Table 2 shows the onset dates for all four defined regions. Onset tends to occur in the SR first, and then occur in the WR, SACZ region, and finally the ER. In addition to having the greatest overall SLP, the SR also tends to have the earliest onset.

Region:	WR	ER	SACZ	SR
Onset Pentad:	58	68	61	53

Table 2: Average Onset dates for Defined Regions. From NR10.

For potential temperature (Figure 11b), the WR and the ER show an increase in potential temperature between pentads 40-60, but the ER shows a slight delay in the timing of this increase. This is consistent with the results from the study of Li and Fu (2004), as well as consistent with an onset delay in the ER compared to the WR (Table 2). They notice a slight increase of potential temperature around pentads 40-60, much like what is shown in Figure 11b. In Figure 11b, the potential temperature graph for the south region is very different from the other regions. Potential temperature decreases rapidly during the winter pentads and then increases rapidly into the summer pentads. This is due to the latitude at which the SR is located. During the winter, subtropical highs dominate the area near the SR, increasing SLP and lowering potential temperature. As the sun warms the atmosphere during the summer months, the subtropical highs shift slightly to the east, raising the potential temperature near the SR.

In addition to potential temperature, the results found in Figures 11c and 11d are in good agreement with Li and Fu (2004) for sensible and latent heat fluxes. They as well found a decrease in sensible heat and an increase in latent heat as the SH seasons changed from winter to summer. Furthermore, the SACZ region's latent (sensible) heat flux shows a large increase (decrease) during the transition from winter to summer season. During the winter months the surface temperature stays above the temperature of the local atmosphere, which keeps sensible heat flux higher than the latent heat flux. Latent heat flux is high when the surface specific humidity is high, particularly after it just rains. Also, the decrease in difference between the surface temperature and the temperature of the local atmosphere decreases sensible heat flux. This occurs during the transition from winter to summer. These differences in atmospheric conditions show regional variability within the four regions. Furthermore, there is a delay of onset between the WR and the ER shown by the lag of the ER graph in the potential temperature (11b), sensible (11c) and latent heat flux (11d) in Figure 11 and in Table 2. There is also a delay in the SACZ onset compared to the WR clearly shown in the potential temperature (11b) and sensible heat flux (11c) delay of a few pentads in the SACZ region. The NCEP/NCAR atmospheric data conclude that there is a lag between the WR and the SACZ region.

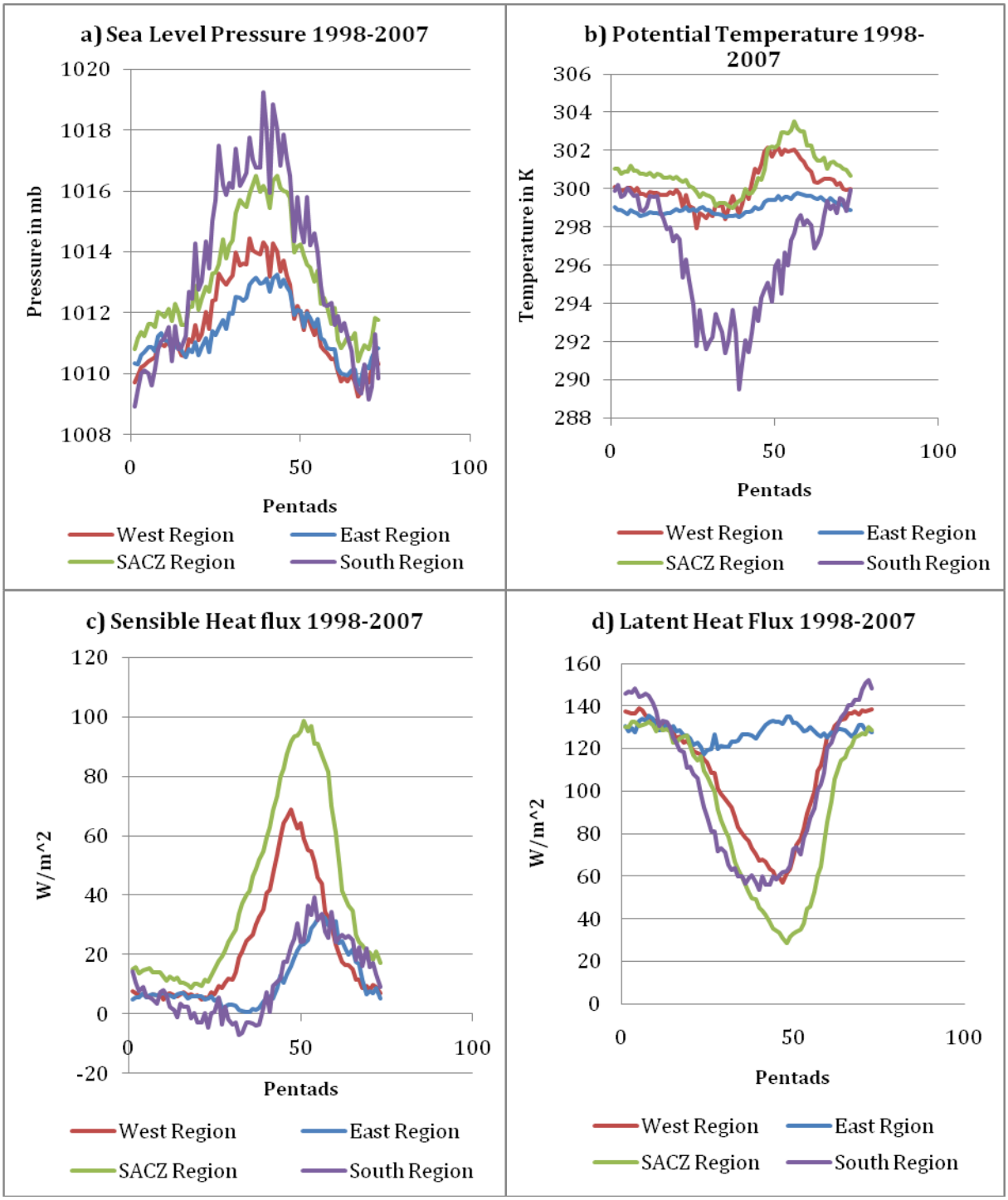

Figure 11: Plots of Regional Variability with NCAR/NCEP data between 1998-2007 including NCEP/NCAR variables of SLP (in mb) (a), Potential Temperature (in Kelvin) (b), Sensible Heat flux (W/m^2) (c) and Latent Heat flux (W/m^2) (d).

To further analyze this lag, the WR and the SACZ were correlated based on NCAR/NCEP atmospheric variables to quantify the lag itself. Figure 12a shows the cross-correlation function of SLP between the WR and the SACZ. The bar graphs represent the correlation coefficient vs. the lag number. The lag number is in pentads, so if the lag between the WR and the SACZ is 3, the WR precedes the SACZ by three pentads in that particular variable. The highest correlation coefficient corresponds to the dominant lag between the regions. For SLP (12a), the bar graph shows high correlations for all lags, but there is a very slight offset towards the positive lag numbers. The dominant lag number (the lag with the highest correlation) is at 0 pentads. This suggests that SLP does not show a lag between the WR and the SACZ. For potential temperature (Figure 12b), there are a greater number of high correlation values within the positive lag numbers meaning there is more of a lag present between the two regions. The highest correlation for potential temperature is indeed at 4 pentads, which suggests that for potential temperature, the SACZ region sees changes in potential temperature 4 pentads after the WR. For sensible heat flux (12c), there is less of an offset of the high correlation values, but the highest correlation value is at +1 pentad. Latent heat flux (12d) shows a similar graph as sensible heat flux, with the highest correlation value also at +1 pentad. The reanalysis data can't model the fluxes as well as, for example potential temperature, which may be the reason for the shift in lag towards 0 pentads. However, both fluxes show a lag in the graphs. For specific humidity, (12e), the correlation values take on more of a normal curve, with the highest correlation value being +1 pentad. Specific humidity might not play as a large of a role in the variability of monsoon onset as previously thought. Finally, volumetric soil moisture (13f) shows a fairly normal curve of the correlation values, and does have a lag of 0.

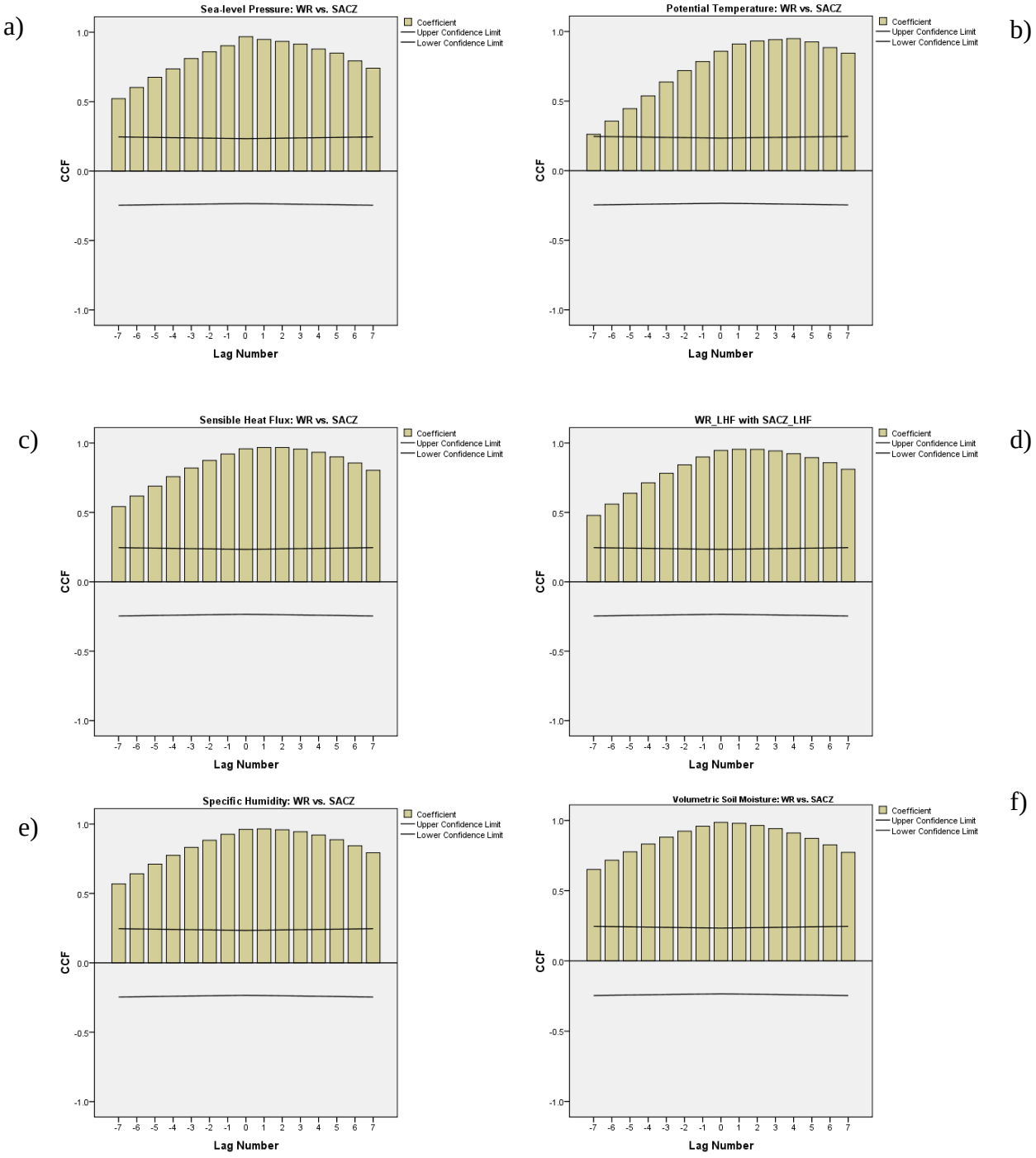

Figure 12: Cross-correlation function between the West Region and the SACZ Region of a) SLP, b) Potential Temperature, c) Sensible Heat Flux (SHF), d) Latent Heat Flux (LHF), e) Specific Humidity, and f) Volumetric Soil Moisture. CCF is the correlation value between the two regions, and lag number is in pentads.

4c. Pre-Onset, Onset, and Post-Onset Cold front Composites

It is also important to look at the daily evolution of cold fronts before and during the monsoon onset pentad to see if there are any significant differences in the evolution or structure of the cold fronts that pass through the region. The third principal component (PC3) of the REOF analysis by NR10 is used to determine monsoon onset in the SACZ region. For the SACZ region, the average onset for 1998-2008 was determined to be at pentad 61 (Table 1). Cold front composites were constructed for cold fronts that occurred before, during, and after onset for the SACZ region. Figures 13, 14 and 15 are composites of GPCP rain and 200 mb geopotential height anomalies. Figure 13 shows the composite for the last cold front that occurred before the SACZ onset pentad for 1998-2008 (hereafter the "pre-onset" cold front). Figure 11 shows the 1998-2008 composite for the cold front that occurred during onset (hereafter the "onset" cold front). Figure 12 shows the composites for the first cold front that occurred after onset (hereafter the "post-onset" cold front). Each figure displays the evolution of cold fronts as they pass through the continent. Day 0 represents the day when the cold front is present in the SACZ region. The plots extend from Day -2 to Day +3 to understand the daily progression of these composite cold fronts.

During "pre-onset" (Figure 13) the composite cold front sweeps through the continent but never makes it to the SACZ region. The cold front is established just south of the SACZ region for a few days and is off the continent by Day +3 (Figure 13f). Intense rainfall in the subtropics in Days -2 and -1 (13d and 13e) indicates the possible presence of Mesoscale Convective Complexes (Velasco and Fritsch, 1987) at that time.

In the WR, there are patterns of convection that show steady rain throughout the "pre-onset" time series in Figure 13 an indicator that the monsoon onset has already occurred (Pentad

58; Table 2) in the WR region. Onset in the WR region is triggered by the slow changes in the thermodynamic conditions of the atmosphere seen in Figure 11 (NR10). Figure 14 shows the 'onset' composite cold front move across the SACZ region. However, the composite cold front becomes stationary and stays in the region until well after Day +3 (Figure 14f). In addition, upper-level negative geopotential height anomaly composites are not only stronger but also more zonally oriented during the "onset" cold front composite indicating a transition to a new regime with more strongly anticyclonically sheared midlatitude cyclones as the SACZ becomes established (Thorncroft et al., 1993). This behavior is unlike the "pre-onset" cold front of Figure 10 based on the orientation and the speed of the composite cold fronts. "Post-onset" (Figure 15) shows similar characteristics as the "onset" composites. The convection in the "post-onset" composites is comparable to the "onset" composites for the SACZ region, but the geopotential height anomalies in the "post-onset" composites tend to be weaker especially as the cold front has passed through the SACZ region. The composite cold front that passes through the SACZ region at Day 0 (15c) again becomes stationary through Days +1 to +3 (15 d, e, f) during "post-onset". Therefore, onset in the SACZ region is likely due to the presence of stationary cold fronts within the region.

Additional composites of various atmospheric variables were also produced. For example, Figure 13 shows the "pre-onset" composites for GPCP rain and sea-level pressure anomalies. At Day -1 (16b), there is an area of negative SLP anomalies present as well as strong convection just south of the SACZ region that is possibly associated with the occurrence of mesoscale convective complexes (MCCs) in Uruguay. Thus there is a possibility that the MCCs are involved in helping with cyclogenesis in that region. As the cold front passes through the SACZ region on Day 0 (16c), there is an area of negative SLP anomalies in the western portion

of the SACZ. The negative SLP anomalies pass through just south of the SACZ region and have exited the continent by Day +2 (16e). During “onset” composites, (Figure 17) there is an area of negative SLP anomalies that appears at about 20˚S on Day -2 (17a). However, as the cold front approaches the SACZ region on Day 0 (17c), the negative SLP anomalies are replaced by positive SLP anomalies. This confirms that the composites are actually cold fronts, as indeed, the composites show an increase in SLP after the system has passed, characteristic of a cold front. During “pre-onset”, the anticyclone behind the composite cold front moves quickly offshore, but during “onset”, the anticyclone lingers on the continent before eventually moving offshore. This suggests that the characteristics of the anticyclone behind a cold front also change between “pre-onset” and “onset”, much like the cold front itself. Similar to “onset” composites, progression of the SLP anomalies is shown in Figure 18 of the “post-onset” cold front composite.

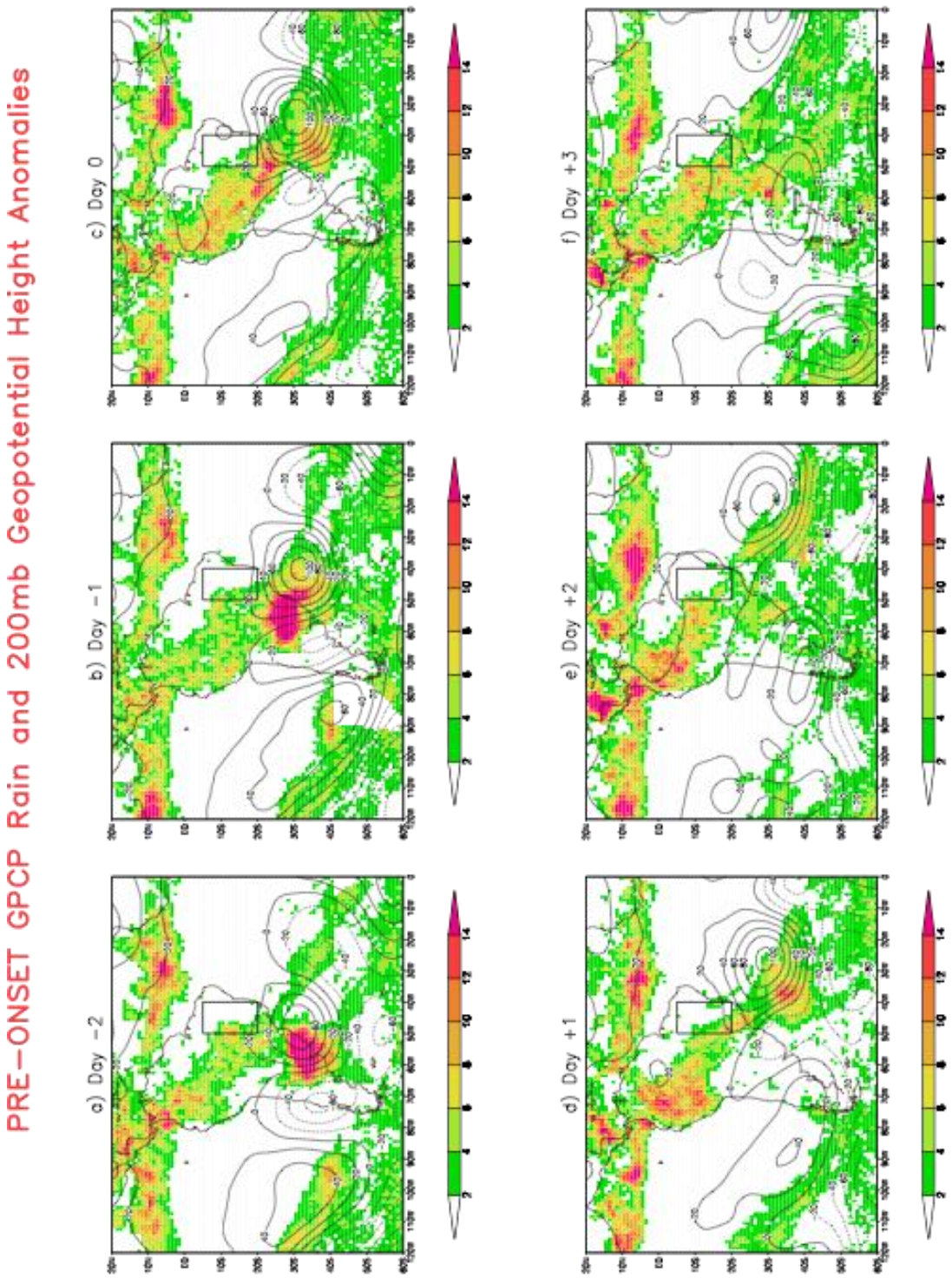

Figure 13: Cold Front Composites for Pre-Onset: Geopotential Height Anomalies (in m) based on NCEP/NCAR reanalysis data.

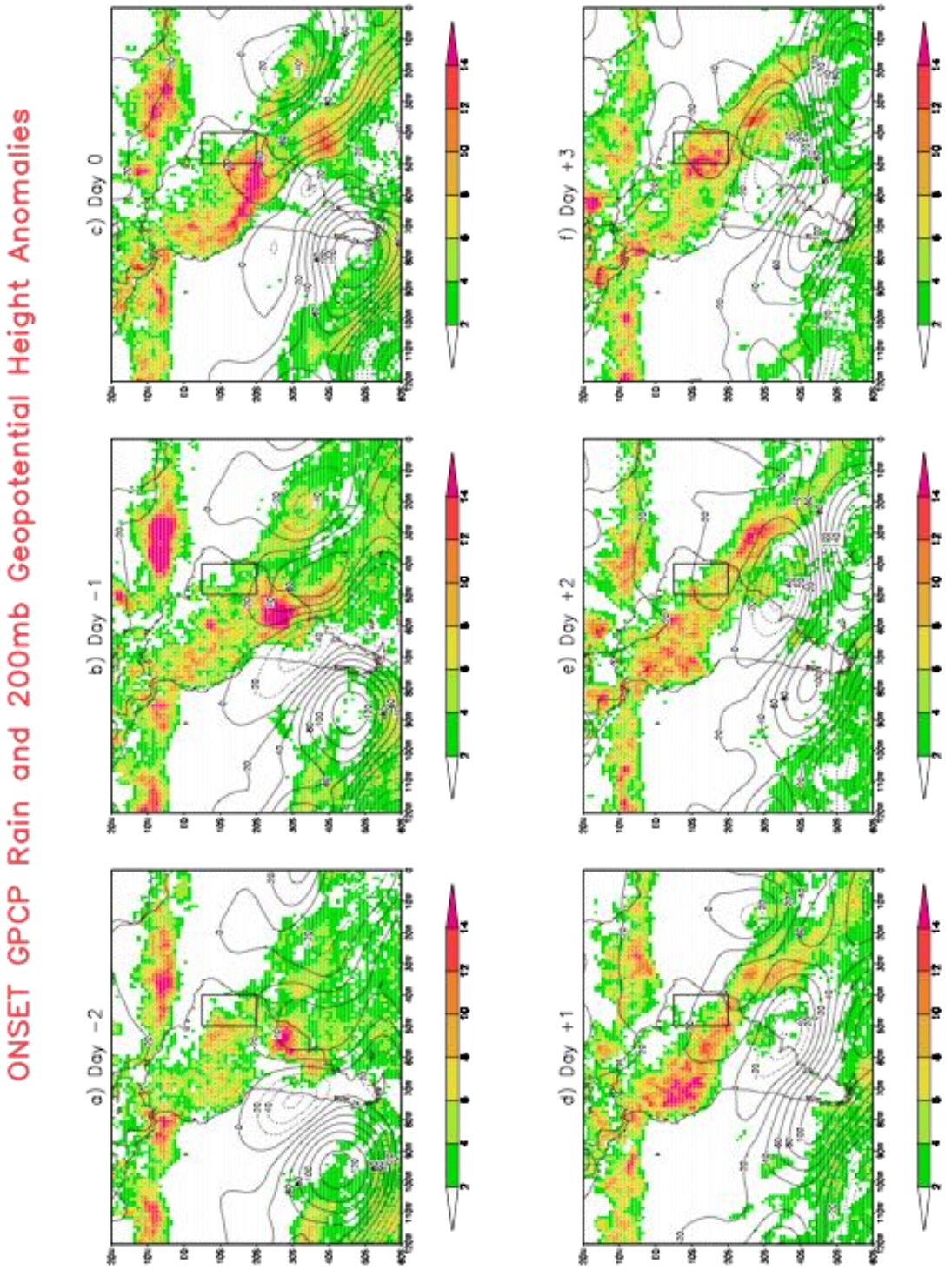

Figure 14: Cold front Composites for Onset: Geopotential Height Anomalies (in m)based on NCEP/NCAR reanalysis data.

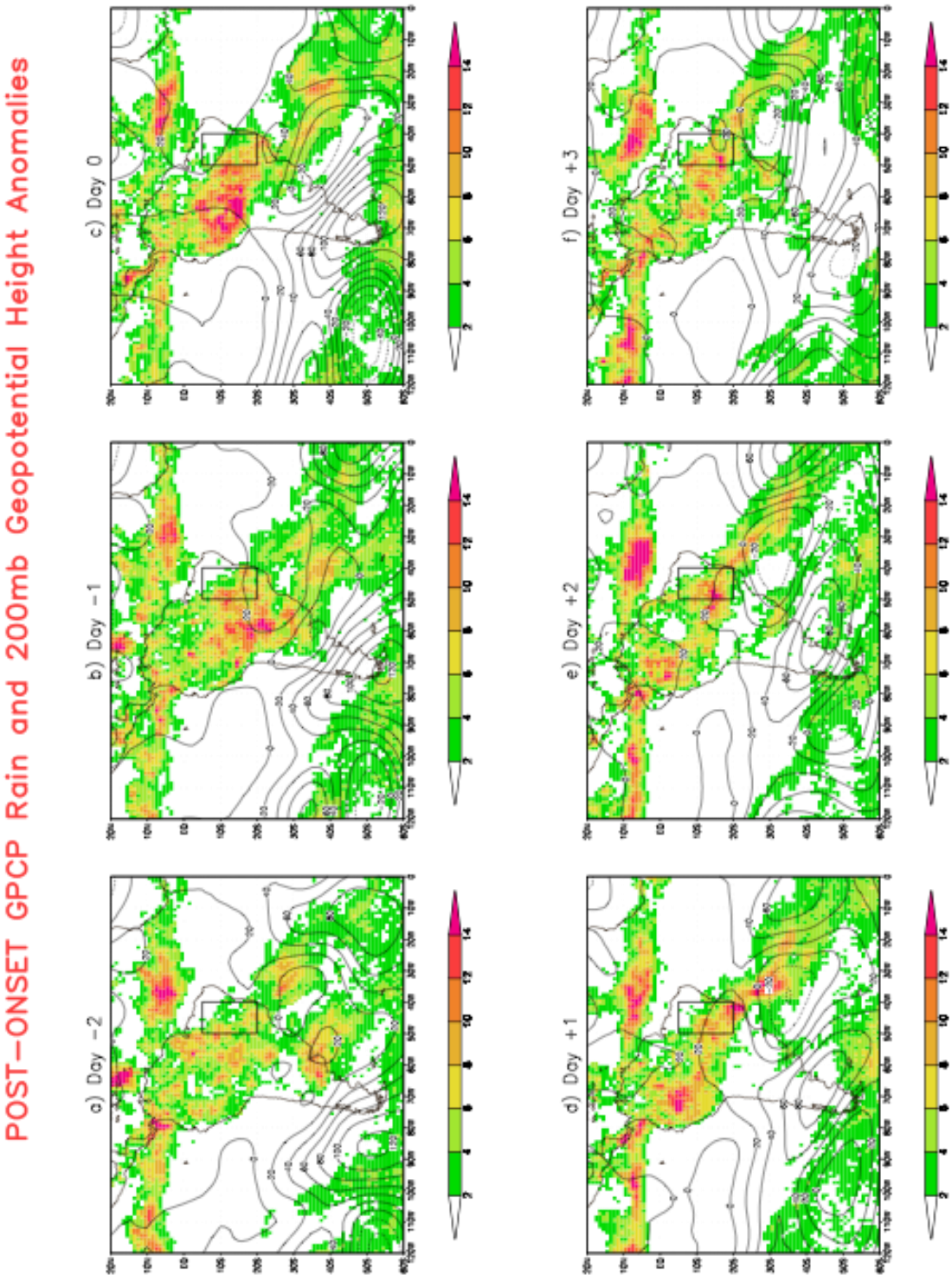

Figure 15: Cold front Composites for Post-Onset: Geopotential Height Anomalies (in m) based on NCEP/NCAR reanalysis data.

Composites of 925mb air temperature anomalies were analyzed for “pre-onset”, “onset”, and “post-onset”. “Pre-onset” cold front composites for air temperature anomalies are shown in Figure 16. At Day 0 (16c), ahead of the composite cold front there is an area of positive temperature anomalies stationed over the SACZ region and behind the composite cold front an area of negative temperature anomalies just southwest of the SACZ region. This is typical for a cold front, which sees warm air ahead of the front and colder air behind the front. This pattern continues as the cold front moves east of the region on Day +2 (16e) and +3 (16f). For “onset” (Figure 17), the same pattern as in “pre-onset” emerges during Day -2 (17a) and Day -1 (17b). The cold front reaches the SACZ region on Day 0 (17c) and becomes stationary at Day +1 (17d). The negative temperature anomalies that were southwest of the SACZ region have expanded into the SACZ region, whereas the positive anomalies that were in the SACZ region on Day -1 have been pushed into the eastern portion of the SACZ region and have disappeared by Day +3. The increase in strength of the negative temperature anomalies means this cold front is bringing colder than average air to the region during onset. Figure 16c shows a strong temperature gradient between the warm air (positive anomalies) preceding the cold front and the cold air behind the front (negative anomalies) during “pre-onset”. During the onset period (Figure 17c), there is a weaker temperature gradient between the warm air in front of the composite cold front and the cold air behind the composite cold front. This pattern of temperature anomalies is also shown in Figure 18 in the “post-onset” composites. The differences in the temperature gradients from the “pre-onset” cold front to the “onset” cold front signals that characteristics of a cold front are changing between “pre-onset” and “onset”. A weaker temperature gradient at onset suggests a weaker cold front or possibly the transition of a cold front into another front, such as a stationary front.

Cold fronts may be influenced by the establishment of the Bolivian High. In the summer months the Bolivian High changes the pattern of the upper-tropospheric westerlies that flow across the continent and thus changes the horizontal tilt of the cold fronts (Silva Dias et al., 1983). The change in tilt could lead to changes in the speed of the cold fronts, which could explain the differences in the speed of cold fronts between "pre-onset" and "onset" composites (Silva Dias 1983, Thorncroft et al. 1993).

The Bolivian High establishes itself based on primarily latent heat of condensation from strong convection already established in the Amazon Basin (Lenters and Cook 1997, Silva 2007 and Silva Dias 1983). The intense rainfall that is occurring at the time of establishment of the Bolivian High means that onset has occurred in the Amazon Basin (WR) (Figure 19).

Figure 19 shows cold front composites for 200 mb streamfunction for "pre-onset". At Day 0 (19c), the Bolivian High is centered over the Western Amazon Basin. This again confirms that there is latent heat of condensation from convection in the Amazon Basin and that monsoon onset has occurred in the WR. However, the Bolivian High becomes more prominent during the "onset" composites in Figure 20. This suggests that an increase in the strength of the Bolivian High may help to slow the progression of the cold fronts during onset, because the strengthening of the Bolivian High from the "pre-onset" composites to the "onset composites" and the slowing down of the composite cold fronts from the "pre-onset" composites to the "onset composites" suggests that as the Bolivian High circulation increases, the speed of the composite cold fronts decreases. Figure 21 shows the composites for "post-onset", which look very similar to the onset composites. The strengthening of the Bolivian High changes the speed of the propagation of the cold fronts through the SACZ region.

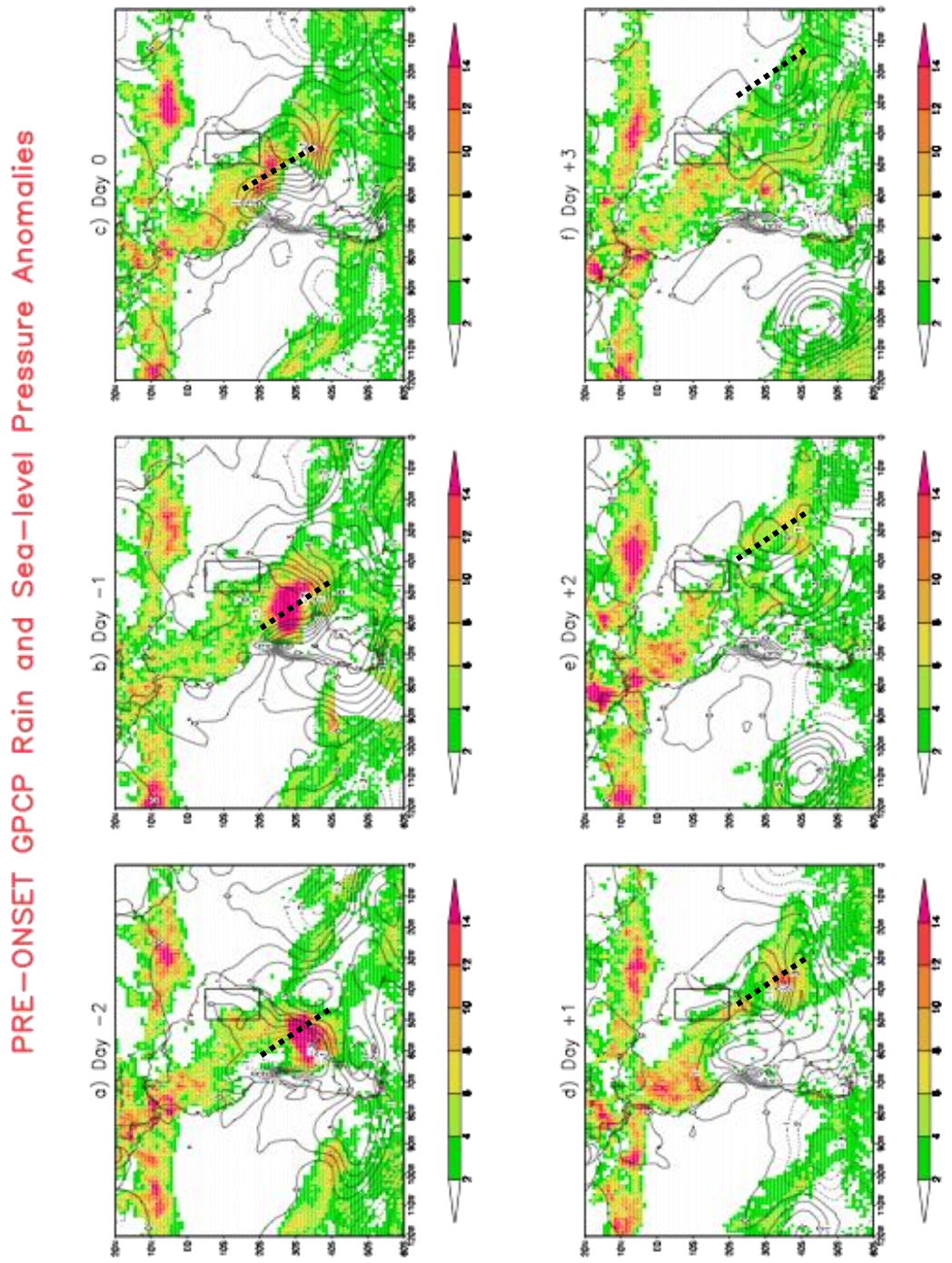

Figure 16: Cold Front Composites for Pre-Onset: SLP Anomalies (in mb) based on NCEP/NCAR reanalysis data.

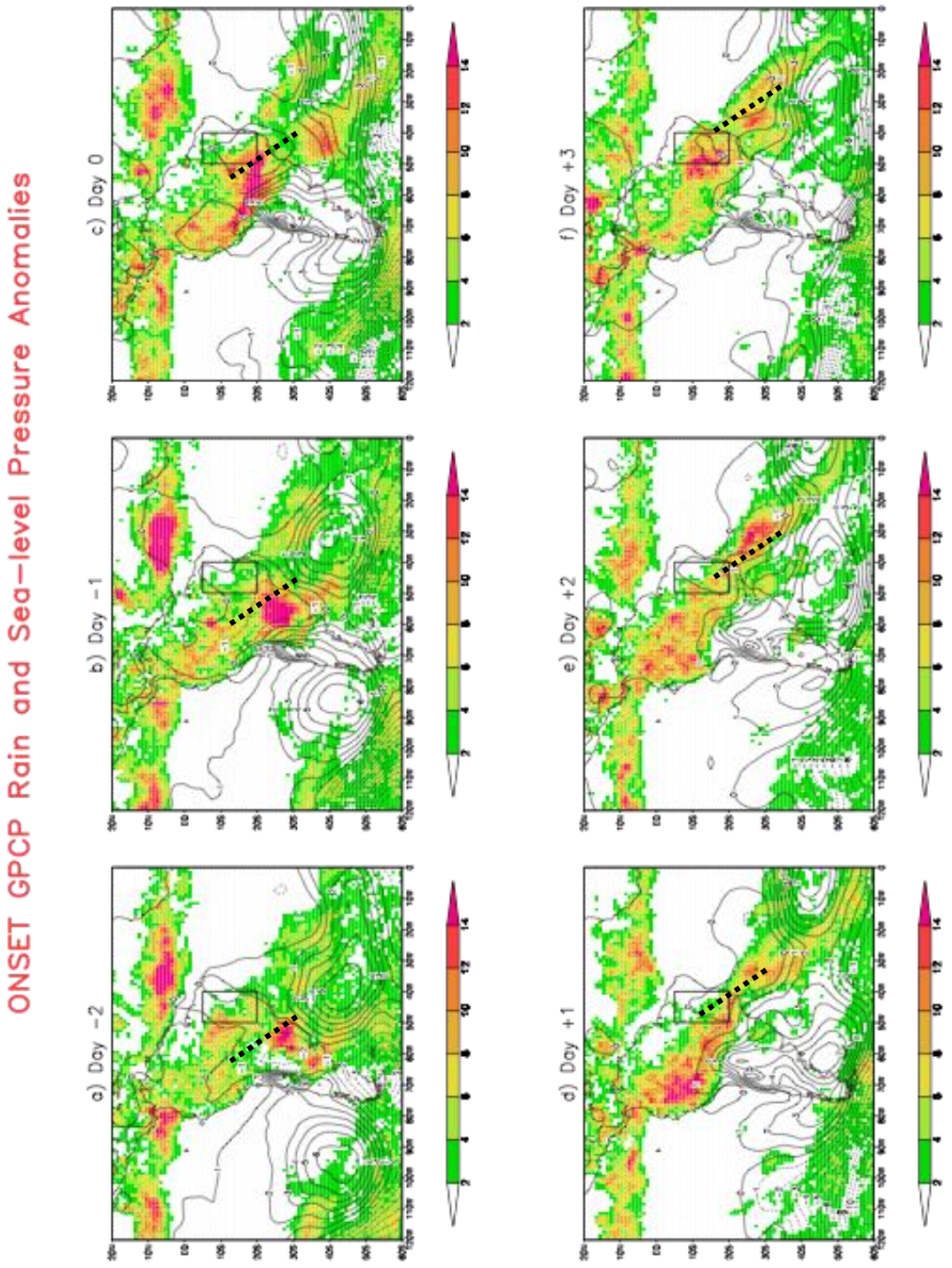

Figure 17: Cold Front Composites for Onset: SLP Anomalies (in mb) based on NCEP/NCAR reanalysis data.

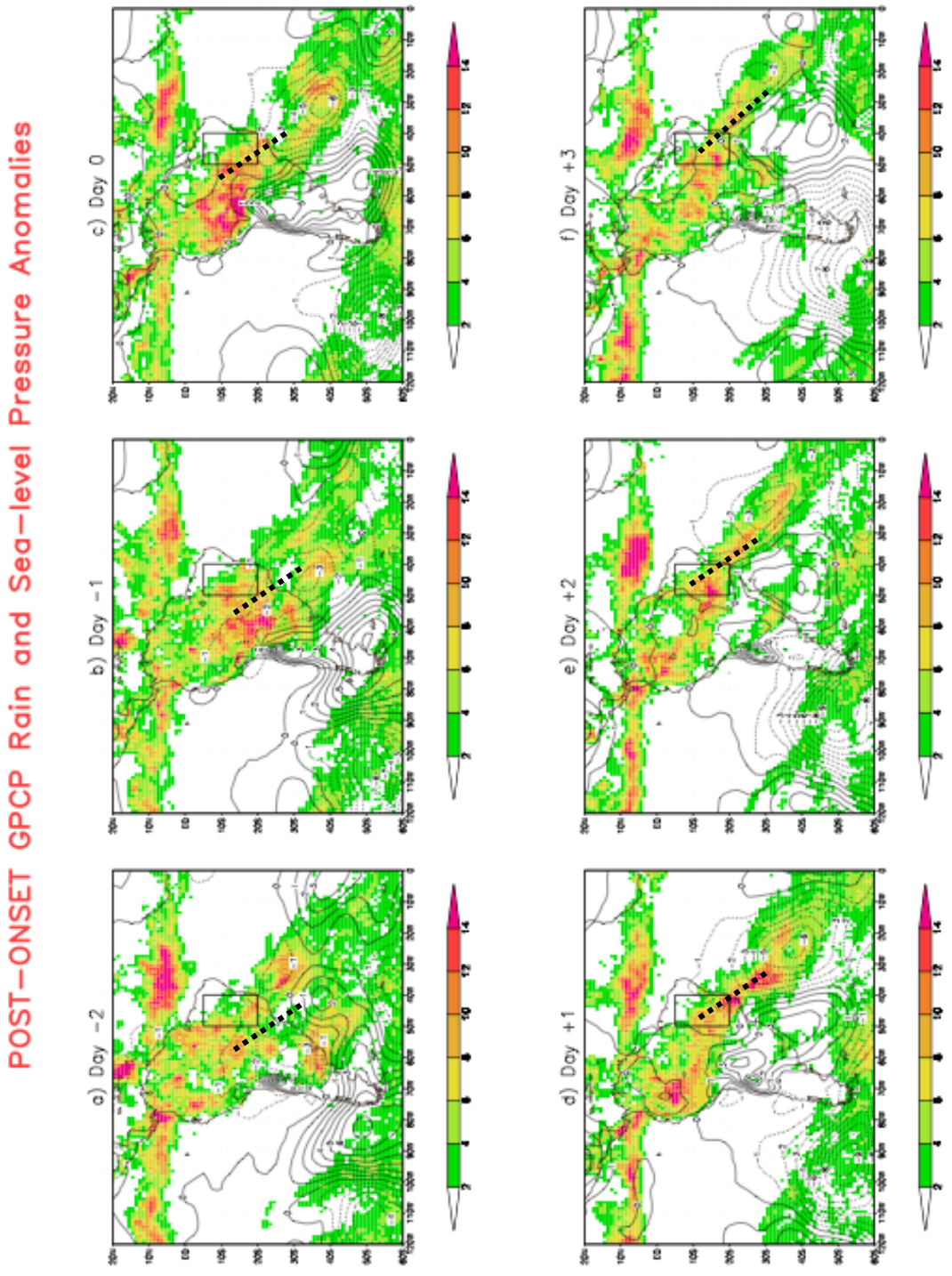

Figure 18: Cold Front Composites for Post-Onset: SLP Anomalies (in mb) based on NCEP/NCAR reanalysis data.

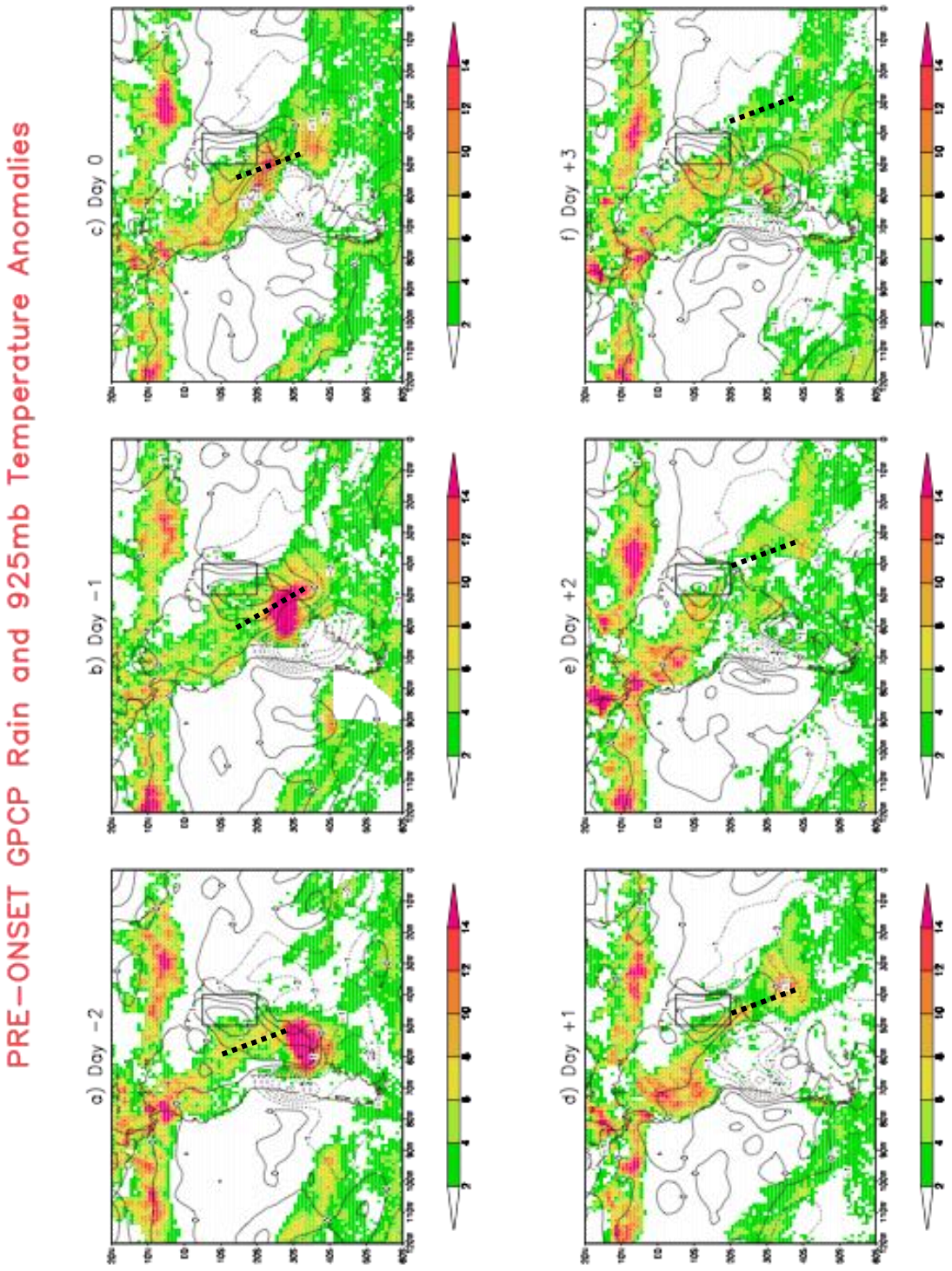

Figure 19: Cold Front Composites for Pre-Onset: Temperature Anomalies (in Kelvin) based on NCEP/NCAR reanalysis data.

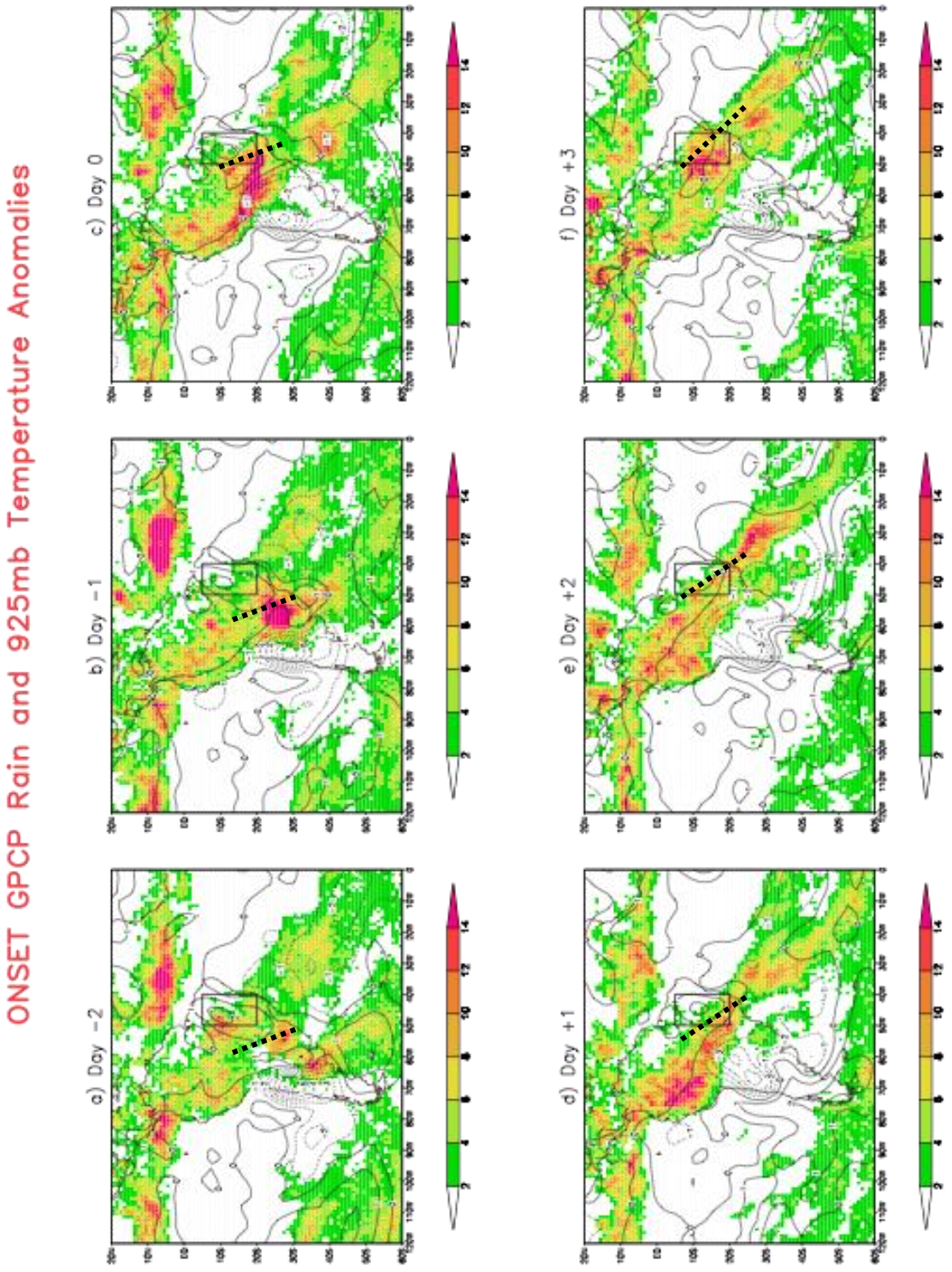

Figure 20: Cold Front Composites for Onset: Temperature Anomalies (in Kelvin) based on NCEP/NCAR reanalysis data.

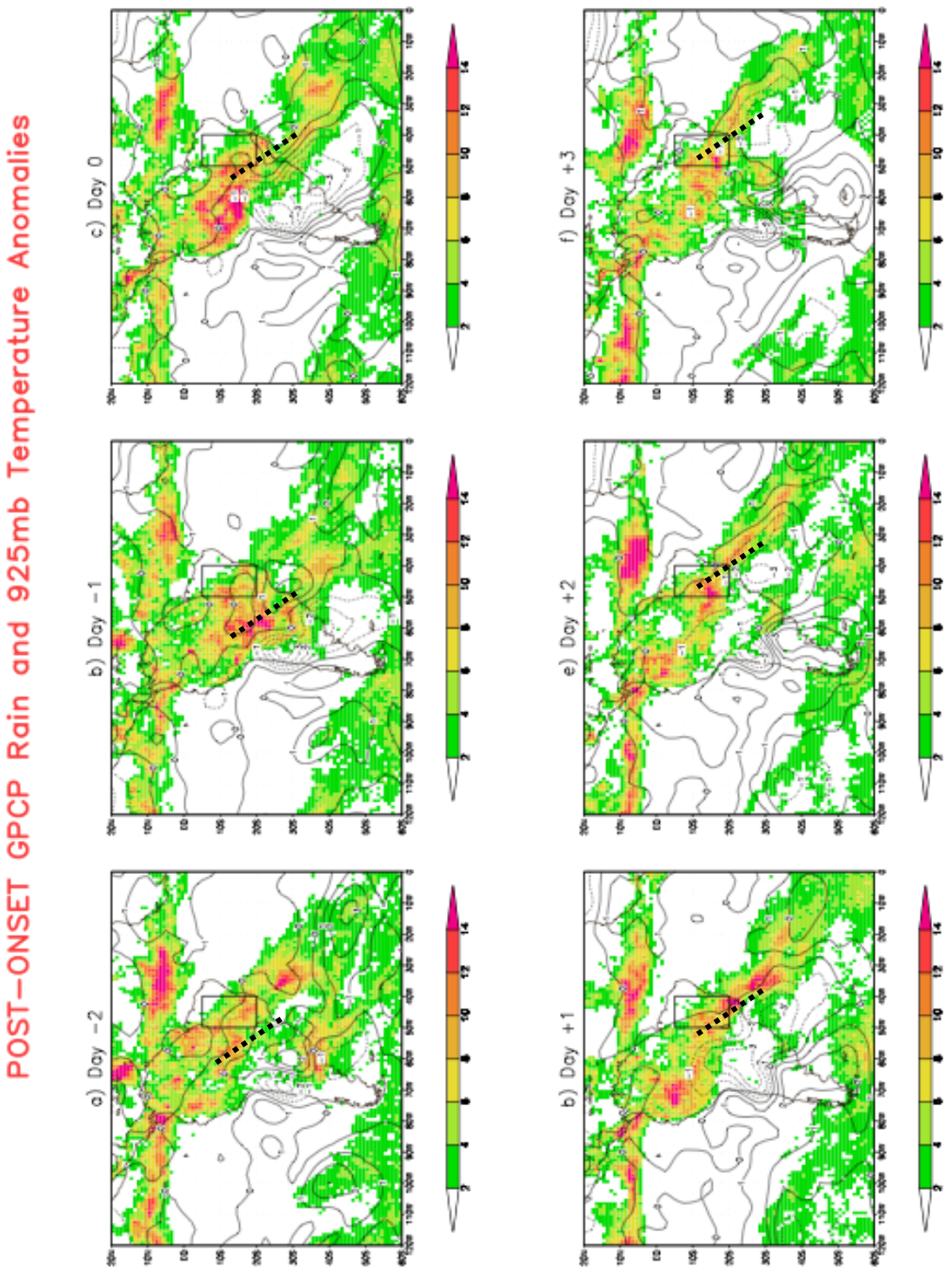

Figure 21: Cold Front Composites for Post-Onset: Temperature Anomalies (in Kelvin) based on NCEP/NCAR reanalysis data.

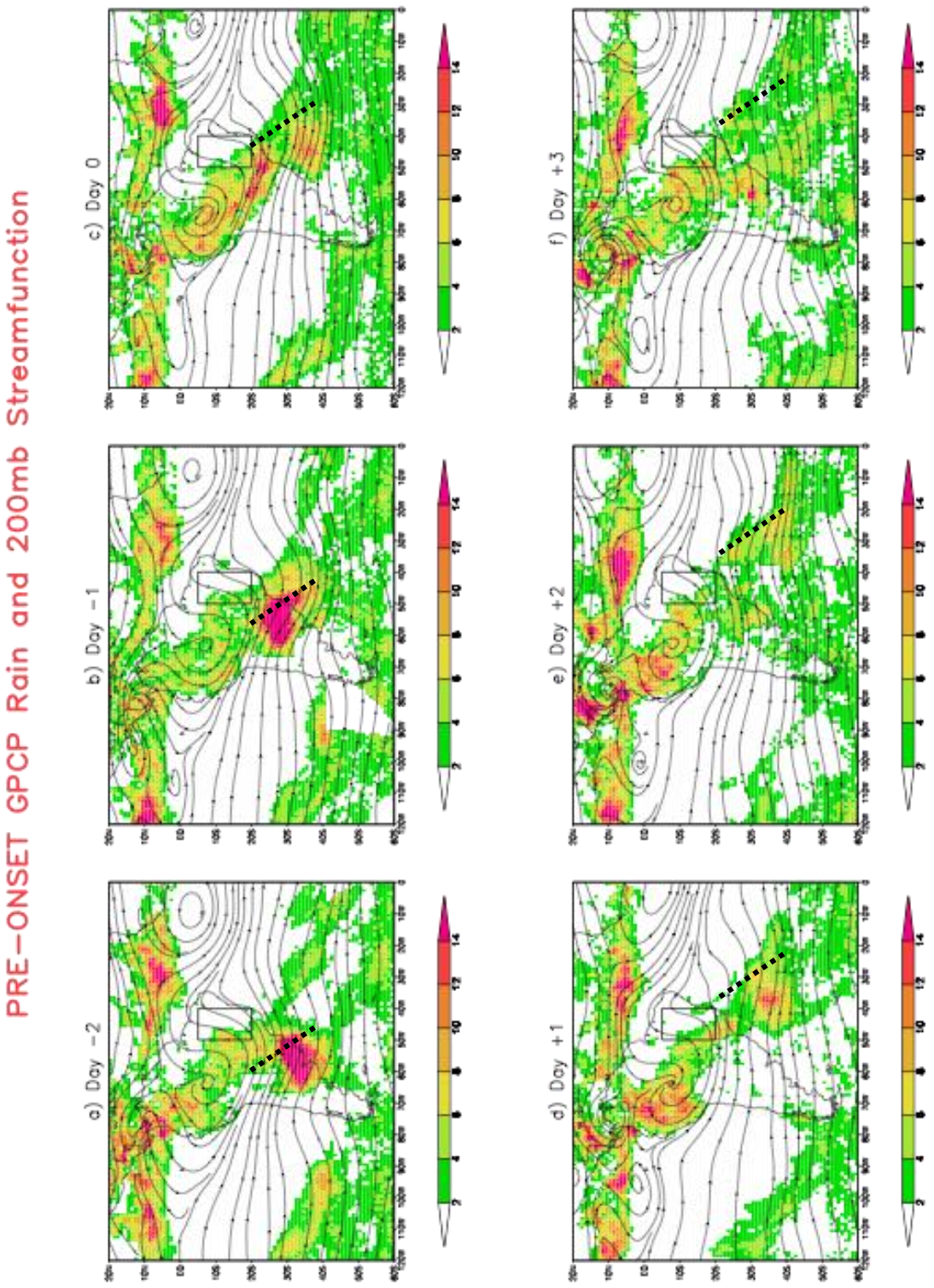

Figure 22: Cold Front Composites for Pre-Onset: 200 mb Streamfunction based on NCEP/NCAR reanalysis data.

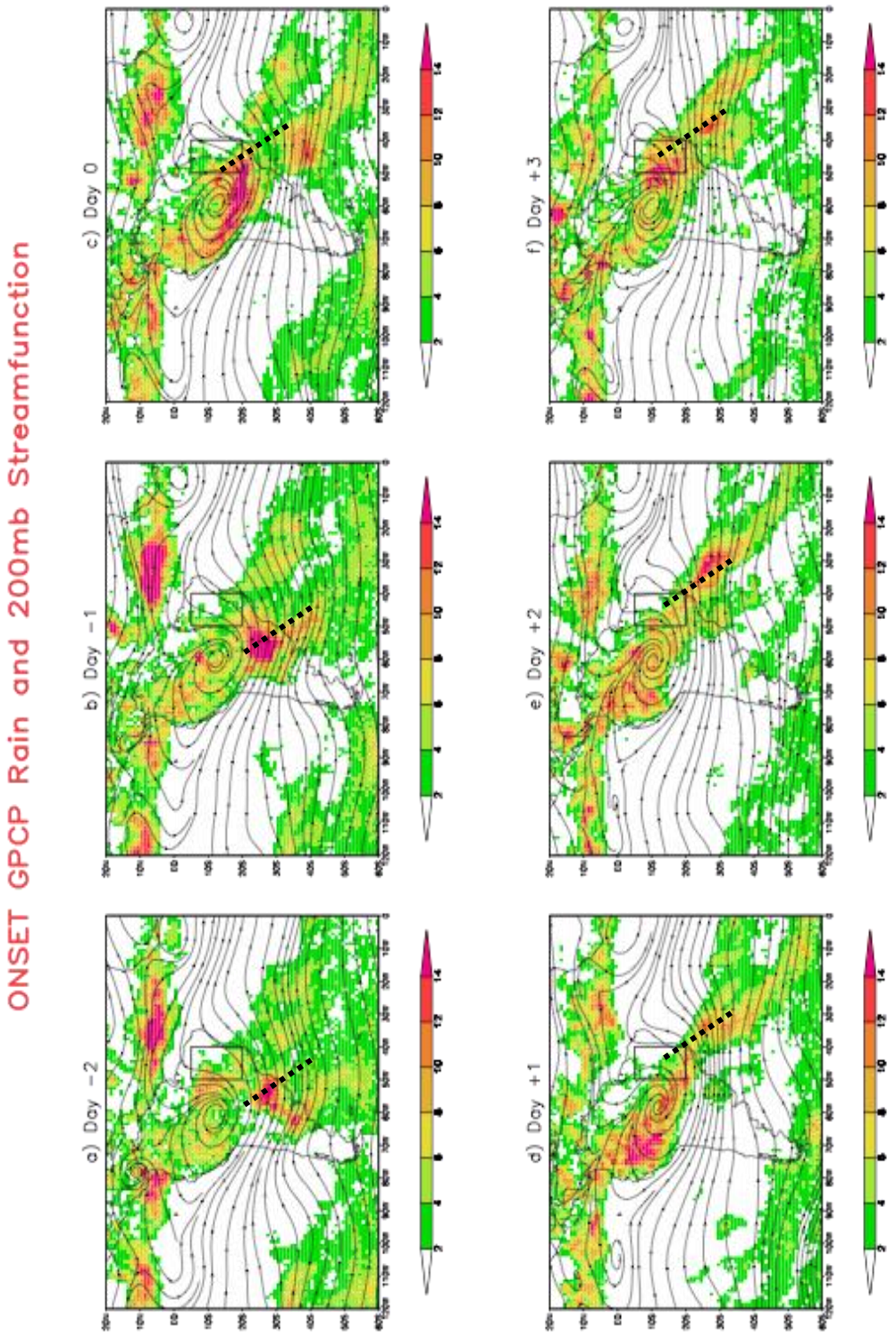

Figure 23: Cold Front Composites for Onset: 200 mb Streamfunction based on NCEP/NCAR reanalysis data.

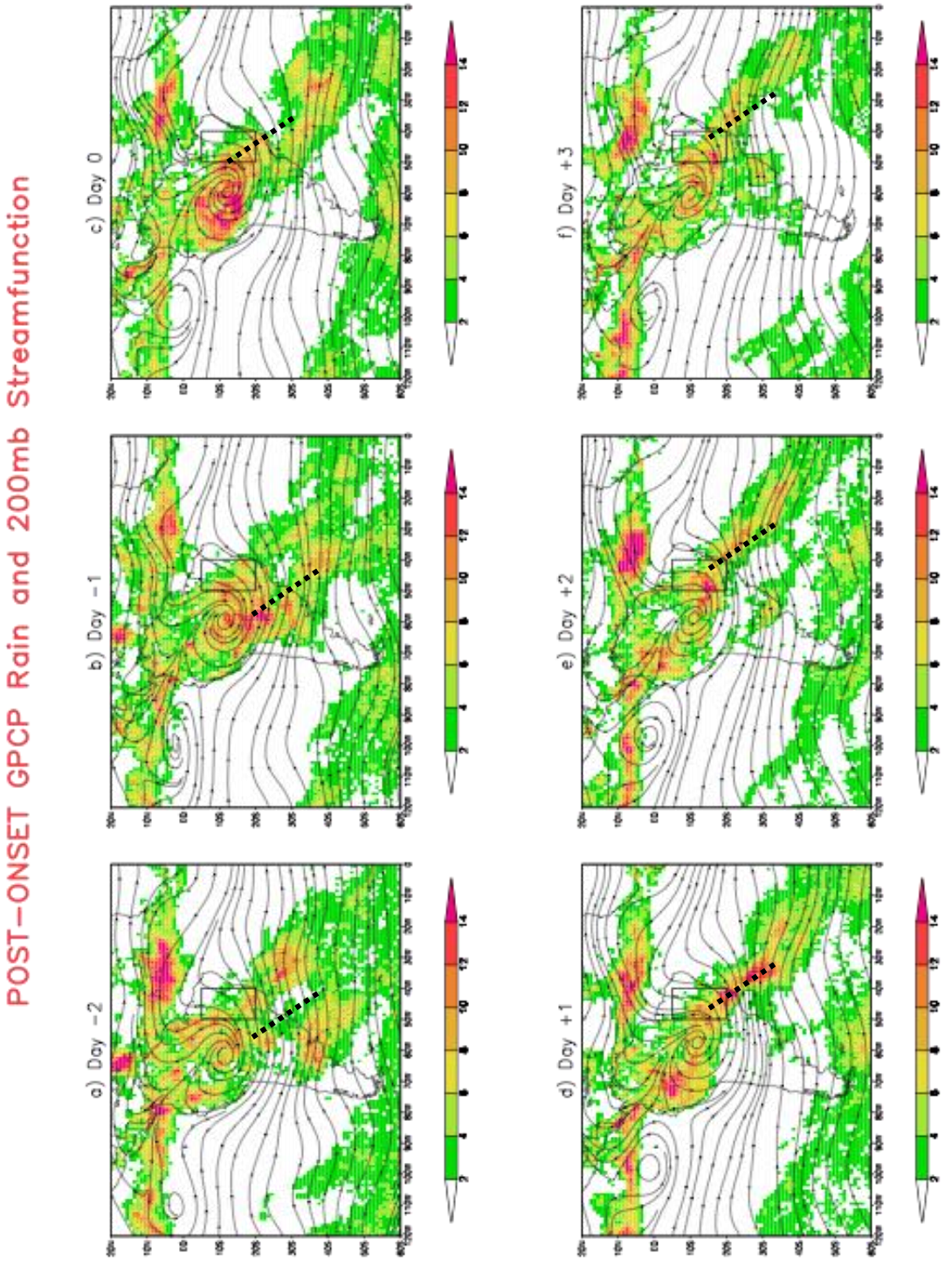

Figure 24: Cold Front Composites for Post-Onset: 200 mb Streamfunction based on NCEP/NCAR reanalysis data.

4d. Comparisons of Normal, Early, and Late Onsets – Latent and Sensible Heat Fluxes

It is important to understand the atmospheric conditions at monsoon onset. Case studies allow for comparison between early and late onsets and normal onsets. This would help understand what variables affect monsoon timing, and how changes in the variables change onset. To do so, a year with an early onset, a year with a late onset, and a year with a normal onset were compared based on sensible heat flux and latent heat flux. The years were chosen based on Table 1. Figure 25 shows sensible heat flux for 2006 (early onset), 2007 (late onset), and 2003 (normal onset) for the SACZ region. For 2003, sensible heat gradually increases between pentads 20 and 50, then decreases rapidly until pentad 70. During 2006, sensible heat increases at pentad 20, but the flux values are smaller than in 2003. It takes longer for the sensible heat flux to reach around the same maximum as in 2003, but only by two pentads (pentad 52). However, the 2006 sensible heat values decrease more quickly between pentads 50-70 and reach a minimum before the values in 2003. For 2007, the opposite is seen; sensible heat values begin to increase gradually at the same time as 2003, but tend to have larger flux values between pentads 20-50 and reach a maximum faster than in 2003. The values continue be the largest of the three years as they rapidly decrease and reaches a minimum before any of the other years. This suggests that a larger sensible heat maximum could lead to a later onset pentad, as high sensible heat values are associated with dry air, therefore there is a lack of convection in the area (Fu, et al. 1999). As the sensible heat flux stays at a maximum, latent heat is at a minimum.

In Figure 26, latent heat flux is displayed for early, late, and normal years for the SACZ region. For all three years, latent heat gradually decreases starting at pentad 10 and reaches a minimum at pentad 50. It then rapidly increases and arrives at a maximum at around pentad 71. For 2006 (early onset), latent heat flux tends to have larger values than the other year as it

quickly increases. For 2007 (late onset), the values tend to be slightly lower as they increase rapidly until pentad 70. Thus increased latent heat values that are higher than during normal onset could show that convection is already in the area before onset. This also is confirmed with the sensible heat flux, where decreasing of sensible heat values more rapid than a normal onset means that convection is established in the SACZ region right before onset. An earlier than normal decrease (increase) of sensible (latent) heat flux could signal an early onset.

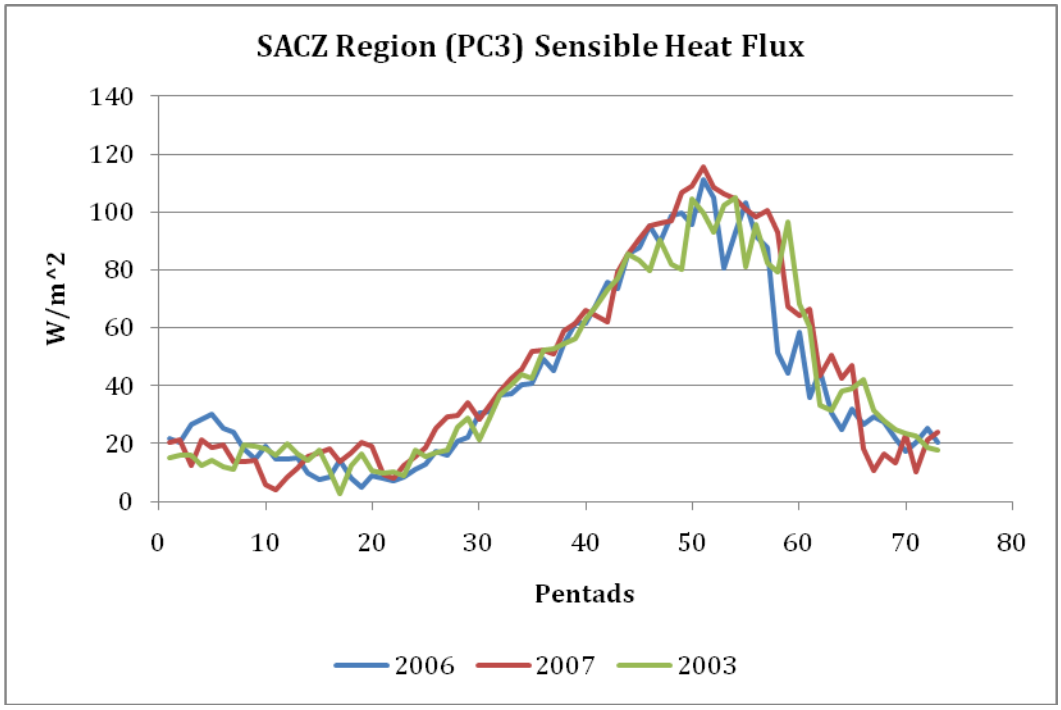

Figure 25: Comparisons of Sensible heat Flux for SACZ Region based on NCEP/NCAR reanalysis data 2003 is a normal onset year, 200 6is an early onset year, and 2007 is a late onset year. Sensible heat flux is in W/m^2.

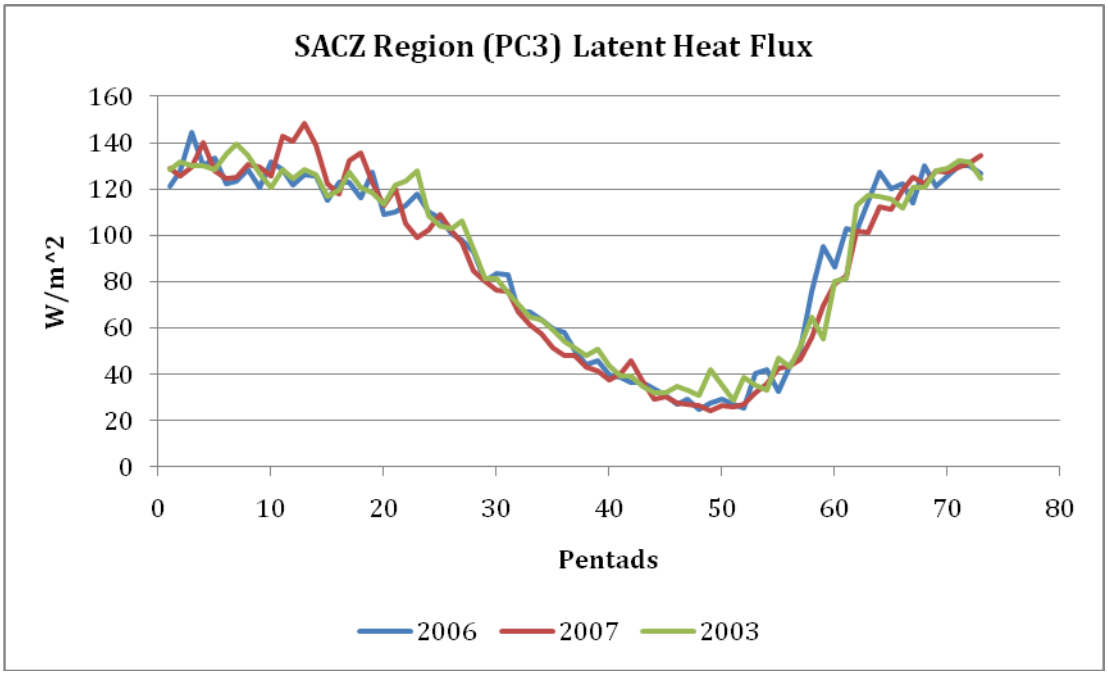

Figure 26: Comparisons of Latent heat Flux for SACZ Region based on NCEP/NCAR reanalysis data. Latent heat flux is in W/m^2.

4e. Comparisons of Normal, Early, and Late Onset Years - Cold Fronts

Another approach to understanding the characteristics of monsoon onset is to analyze atmospheric variables with the dates of cold fronts for the same early, late and normal onset years above. Time series were constructed showing each year (2003, 2006, 2007) with the dates of the 1010 mb threshold cold fronts that passed through South America (as defined in NR10) overlaid on several atmospheric variables. Figure 27 shows 0-10 cm volumetric soil moisture and sensible and latent heat fluxes for 2003. The dashed lines indicate the dates of cold fronts, and the bold line is roughly the center of the monsoon onset pentad in the SACZ region. For the volumetric soil moisture (27a; non-dimensional), the annual cycle is present, showing a decrease in moisture starting in mid April and is at a minimum in late August. By September the volumetric soil moisture is increasing, and levels off a little over a month after onset has occurred in the SACZ region. The increase in volumetric soil moisture is related to rainfall

already occurring in the WR. Figure 28a (early onset) and Figure 29a (late onset) both show similar patterns of volumetric soil moisture. Spikes in volumetric soil moisture shown in Figures 27a, 28a, and 29a are the result of cold fronts bringing precipitation into the region. The cold fronts that contain precipitation contribute to the increase of the volumetric soil moisture right before onset. All three years also show a similar threshold of 0-10 cm volumetric soil moisture at onset (~0.30).

For sensible heat flux during the normal year (Figure 27b), the annual cycle is also present, with an increase during the months of June-October, but quickly decreasing right before onset and reaching a minimum during the monsoon season. The dates of the cold fronts seem to be associated with drops in sensible heat flux, especially within two months before onset. This was found in Gallus and Segal (1999) where differential cloud cover near a cold front reduced solar irradiance to the surface therefore lowered the sensible heat flux and strengthened the temperature gradient across the front. The latent heat flux decreases during the winter months and increases rapidly right before onset, leveling off after onset. The dates of the cold fronts are associated with spikes in the latent heat flux. These spikes could mean that the cold fronts leading up to onset are bringing moisture to the SACZ region.

Furthermore, sensible and latent heat flux patterns for the early onset year are similar to the normal onset year. However, for the late onset year (Figure 29b), the sensible heat flux shows a more gradual decrease right before onset compared to the normal and early onset years. The latent heat flux as well shows a more gradual increase right before onset. The cold fronts associated with the late year, especially right before onset, do not seem to increase latent heat as much as some of the cold fronts that occurred before onset during a normal year. The lack of

cold fronts that would bring precipitation, therefore larger values of latent heat, into the SACZ could contribute to the late onset observed in that year.

The WR was also analyzed for 2003, 2006, and 2007 with NCEP/NCAR reanalysis data and cold fronts. Figure 30 shows the 2003 time series for volumetric soil moisture, and sensible and latent heat flux. The volumetric soil moisture (30a) is at a minimum during the summer months but begins to increase in mid August until onset. There are positive fluctuations in the soil moisture that appear soon after several cold fronts before onset. This validates that cold fronts bring precipitation to the WR. Sensible heat flux (30b) is at a maximum in September, and gradually decreases in late September until onset. Latent heat flux (30c) begins to increase in late September until onset. The increase is a little more rapid than the sensible heat flux, but not as abrupt as one might see in the SACZ region. This gradual increase (decrease) in latent (sensible) heat flux is an indicator of thermodynamic changes within the WR. Next, the years 2006 (Figure 31) and 2007 (Figure 32) were analyzed, and both years showed similar trends in volumetric soil moisture and sensible and latent heat flux as 2003 in the WR. Once again, the gradual thermodynamic change is present before onset. There is an interesting fluctuation in the 2007 plot (Figure 32) around late July that has latent heat flux and soil moisture increasing rapidly and sensible heat decreasing at the same rate. This is most likely due to the three cold fronts that passed through the area in a short amount of time. Therefore, since there was no indication of a rapid increase or decrease in values for sensible heat flux, latent heat flux, or volumetric soil moisture, the trigger of the monsoon onset in the WR is thermodynamic nature, and is brought upon by a gradual increase in convection in the area.

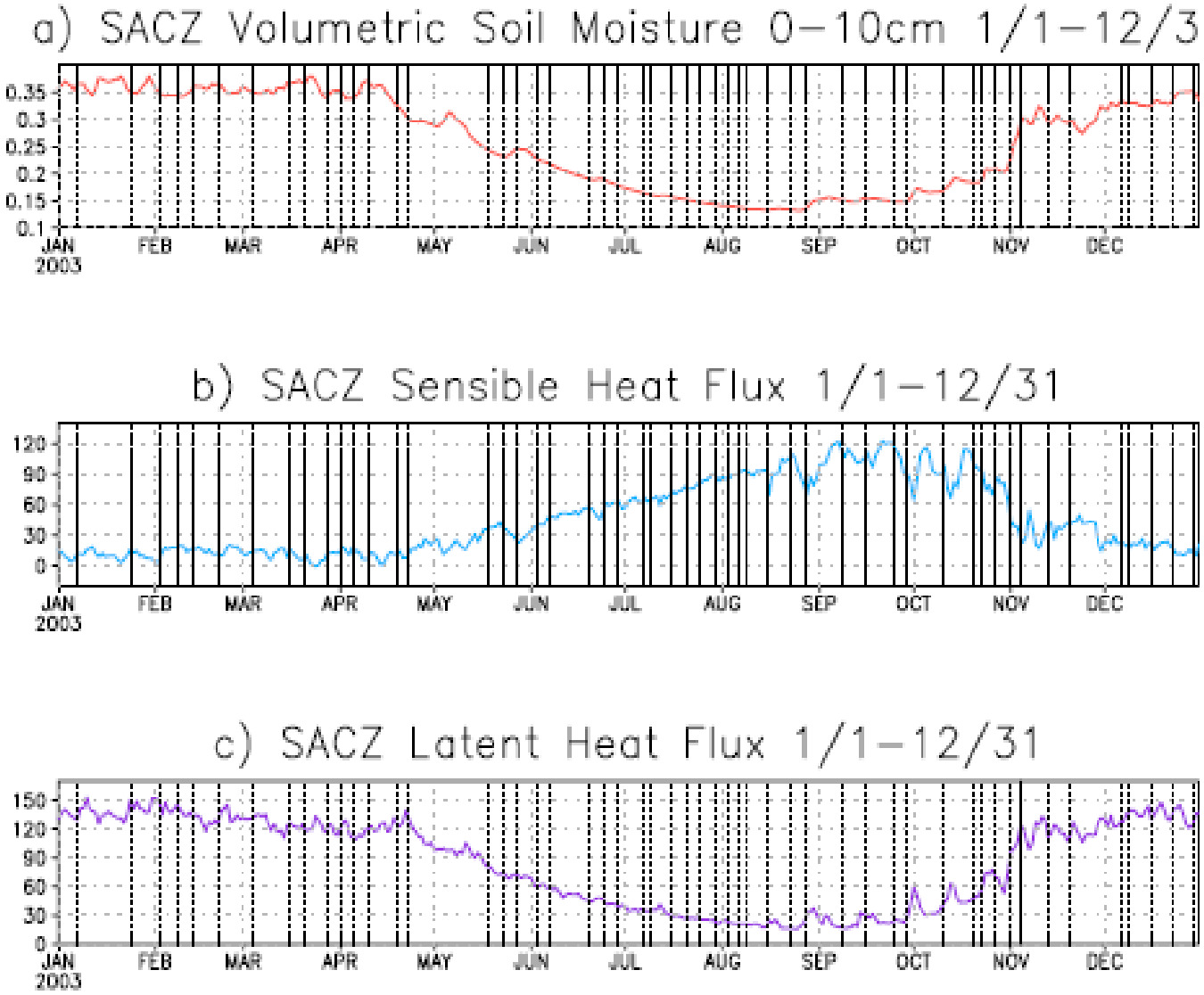

Figure 27: SACZ 2003 Comparisons of 0-10cm Volumetric Soil Moisture (a), Sensible Heat (W/m^2) (b) and Latent Heat flux (W/m^2) (c), (data from NCEP/NCAR) and Cold fronts (dashed lines). Onset is marked with bold line.

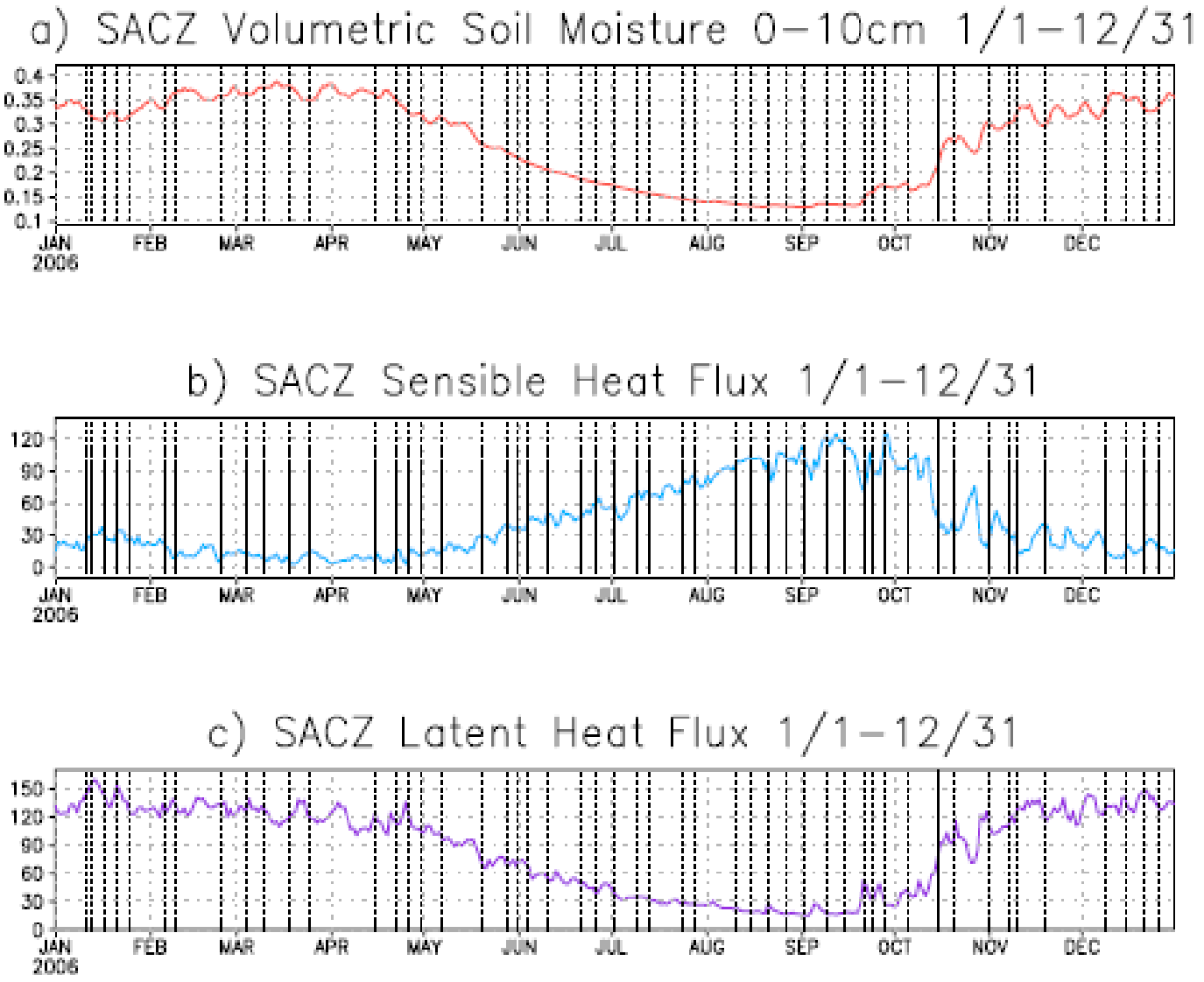

Figure 28: SACZ 2006 Comparisons of 0-10cm Volumetric Soil Moisture (a), Sensible Heat (W/m^2) (b) and Latent Heat flux (W/m^2) (c), (data from NCEP/NCAR) and Cold fronts (dashed lines). Onset is marked with bold line.

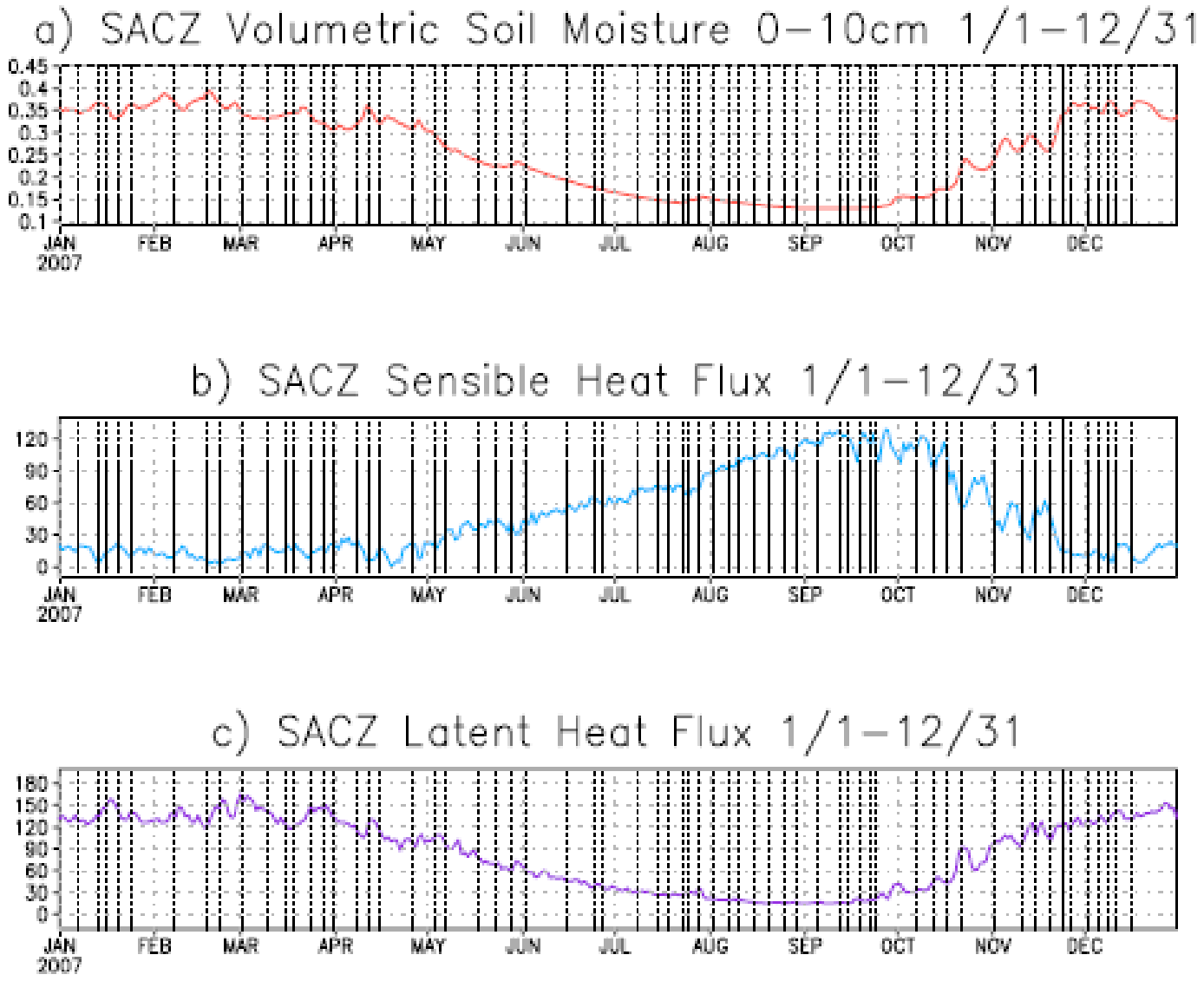

Figure 29: SACZ 2007 Comparisons of 0-10cm Volumetric Soil Moisture (a), Sensible Heat (W/m^2) (b) and Latent Heat flux (W/m^2) (c), (data from NCEP/NCAR) and Cold fronts (dashed lines). Onset is marked with bold line.

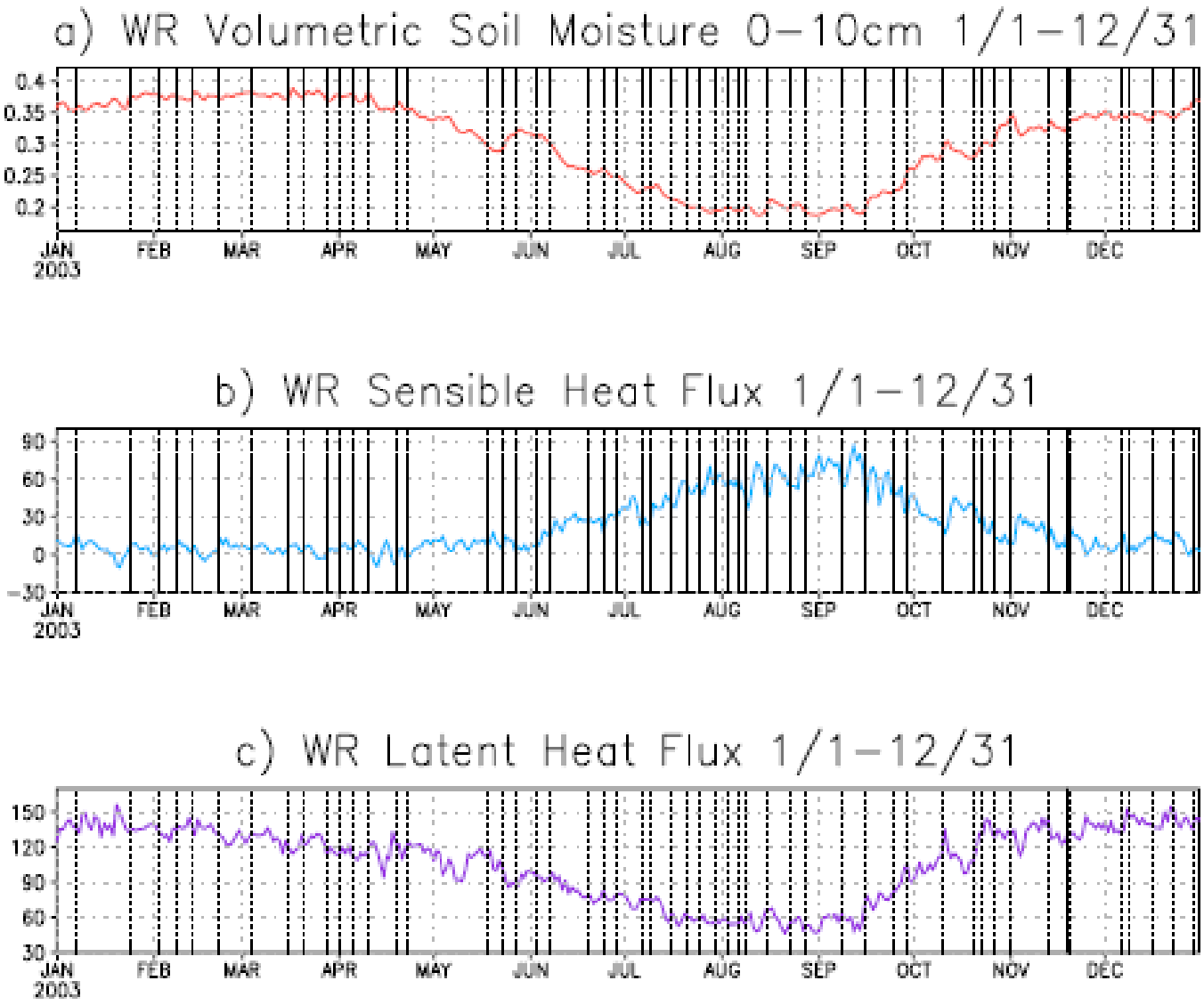

Figure 30: 2003 WR Comparisons of 0-10cm Volumetric Soil Moisture (a), Sensible Heat (b) and Latent Heat flux (W/m^2)(c), (data from NCEP/NCAR) and Cold fronts (dashed lines). Onset is marked with bold line.

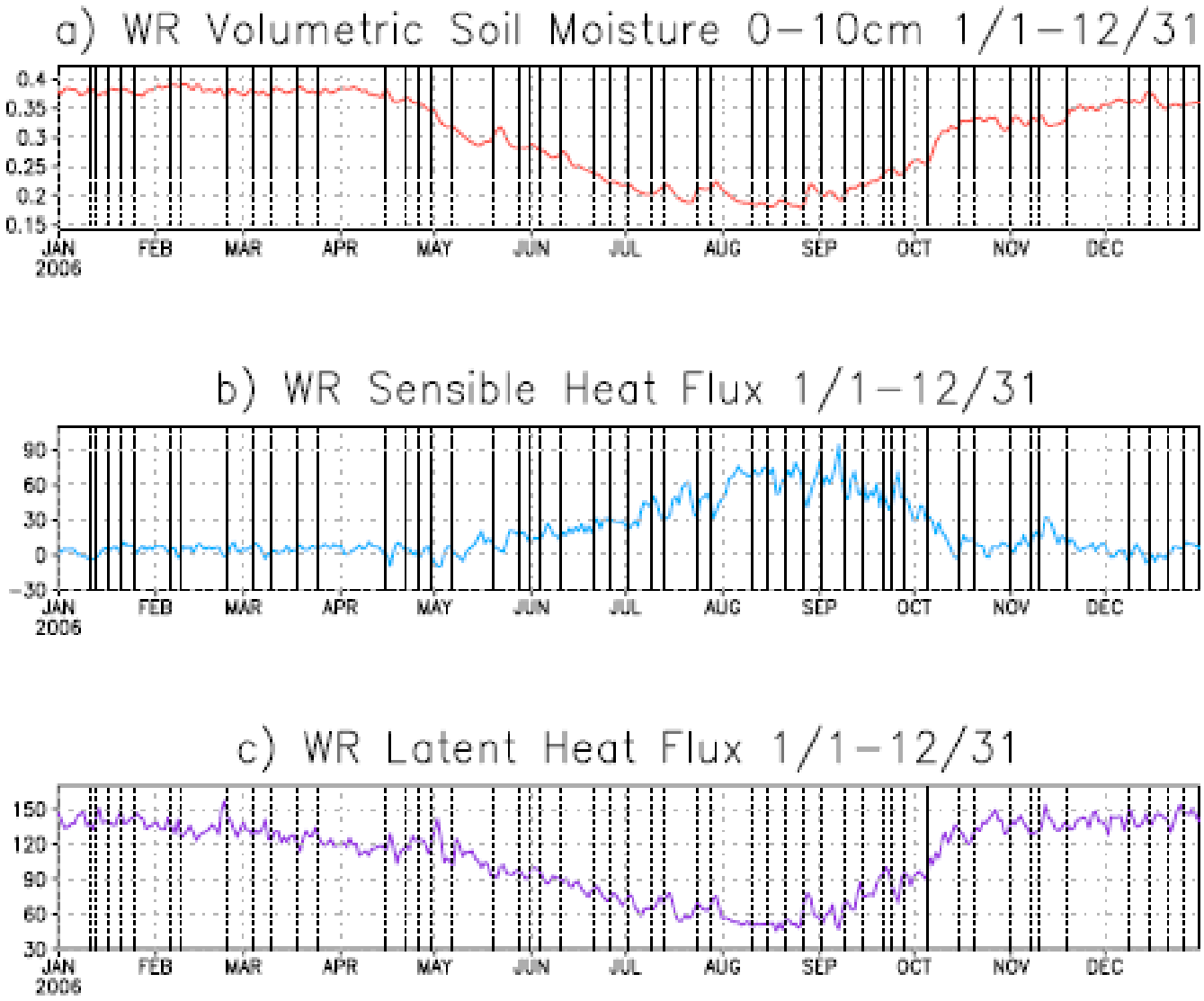

Figure 31: 2006 WR Comparisons of 0-10cm Volumetric Soil Moisture (a), Sensible Heat (W/m^2) (b) and Latent Heat flux (W/m^2)(c), (data from NCEP/NCAR) and Cold fronts (dashed lines). Onset is marked with bold line.

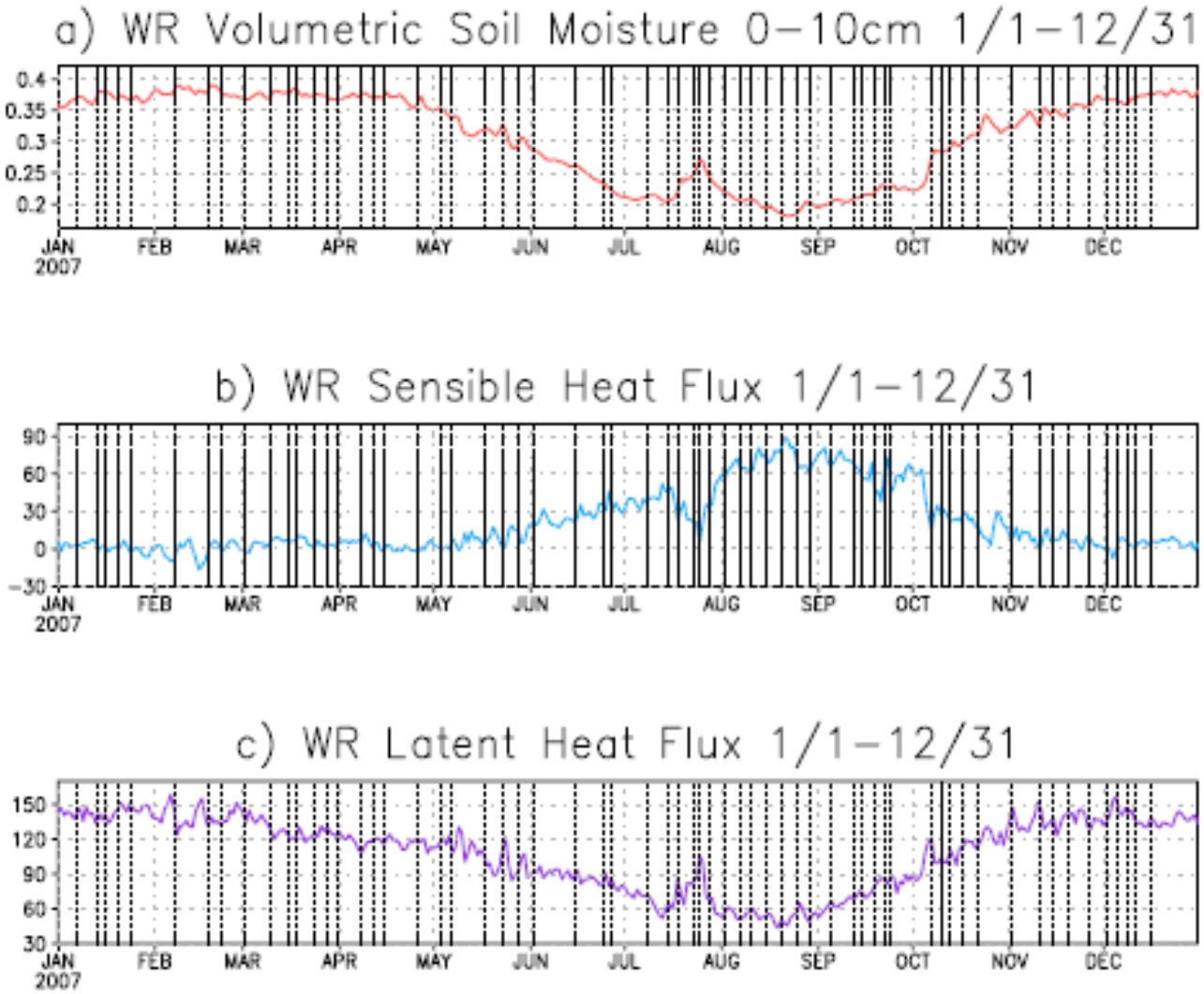

Figure 32: 2007 WR Comparisons of 0-10cm Volumetric Soil Moisture (a), Sensible Heat (W/m^2) (b) and Latent Heat flux (W/m^2)(c), (data from NCEP/NCAR) and Cold fronts (dashed lines). Onset is marked with bold line.

4f. MJO and SAMS Onset:

Following Wheeler and Hendon's analysis of the Indian and Australian monsoon onsets and the MJO phases, MJO phase diagrams were constructed for the WR and SACZ region. Figure 33 shows where the SACZ region onset pentad years for 1979-2008 and fall within the eight phases of the MJO cycle. The mean RMM values for each onset pentad are plotted along the X-axis and Y-axis. The MJO phases are labeled according to Figure 4 (Wheeler and Hendon, 2004). The onset dates for the SACZ region are scattered across the eight MJO phases. For MJO phases 7 and 8, Carvalho et al. (2004) suggested that increased extreme rainfall events in southeastern Brazil were linked to enhanced convective MJO phases in the central Pacific. Figure 33 shows 17 onset years that fell into the "significant" MJO cycle. Only 6 out of those 17 years considered "significant" were within the defined enhanced convective MJO phases (7 and 8) that were linked to monsoon onset. This means about 35% of onset years were within the enhanced portion of the MJO cycle. This is significantly less than the Wheeler and Hendon (2004) analysis of the Australian monsoon, where over 80% of onset years were within the enhanced convection half of the MJO cycle. However, the Wheeler and Hendon (2004) analysis of the Indian monsoon onset determined that there were significantly less onset dates that fell into the enhanced convective phases than in the Australian monsoon analysis. The Indian monsoon onset also did not usually occur during suppressed convective phases (Wheeler and Hendon, 2004) The SACZ region did not necessarily see a cluster of onset years around enhanced convective phases of the MJO cycle like the Indian monsoon, but SACZ monsoon onset did not occur during a South American suppressed convective phase of the MJO, particularly within phase 3. Phase 3, where Wheeler and Hendon (2004) concluded that there was suppressed convection near South America, there were no onset years within that region.

However, since phase 4 was also documented to be a suppressed convective phase for South America, but the MJO did have onset dates within its phase, it is inconclusive that the MJO's suppressed convective phases influence monsoon onset in the SACZ region. In addition, there were no clusters of onset dates within the enhanced convective phases of the MJO. Therefore MJO does not have an influence on the SACZ onset.

For the WR, shown in Figure 34 for comparison to the SACZ region, the onset years are slightly more clustered within phases. Phase 2, which was not a significant enhanced convective phase of the MJO cycle contains several onset years, and Phase 7 contains several onset years as well. Phase 7 is considered an enhanced convective phase of the MJO. In addition, there are no onset years within phase 3 of the MJO, but there are onset dates within phase 4. The WR onset pentad years occur in both enhanced convective phases and in suppressed convective phases, therefore the variability of the WR onset is not likely to be influenced by the MJO.

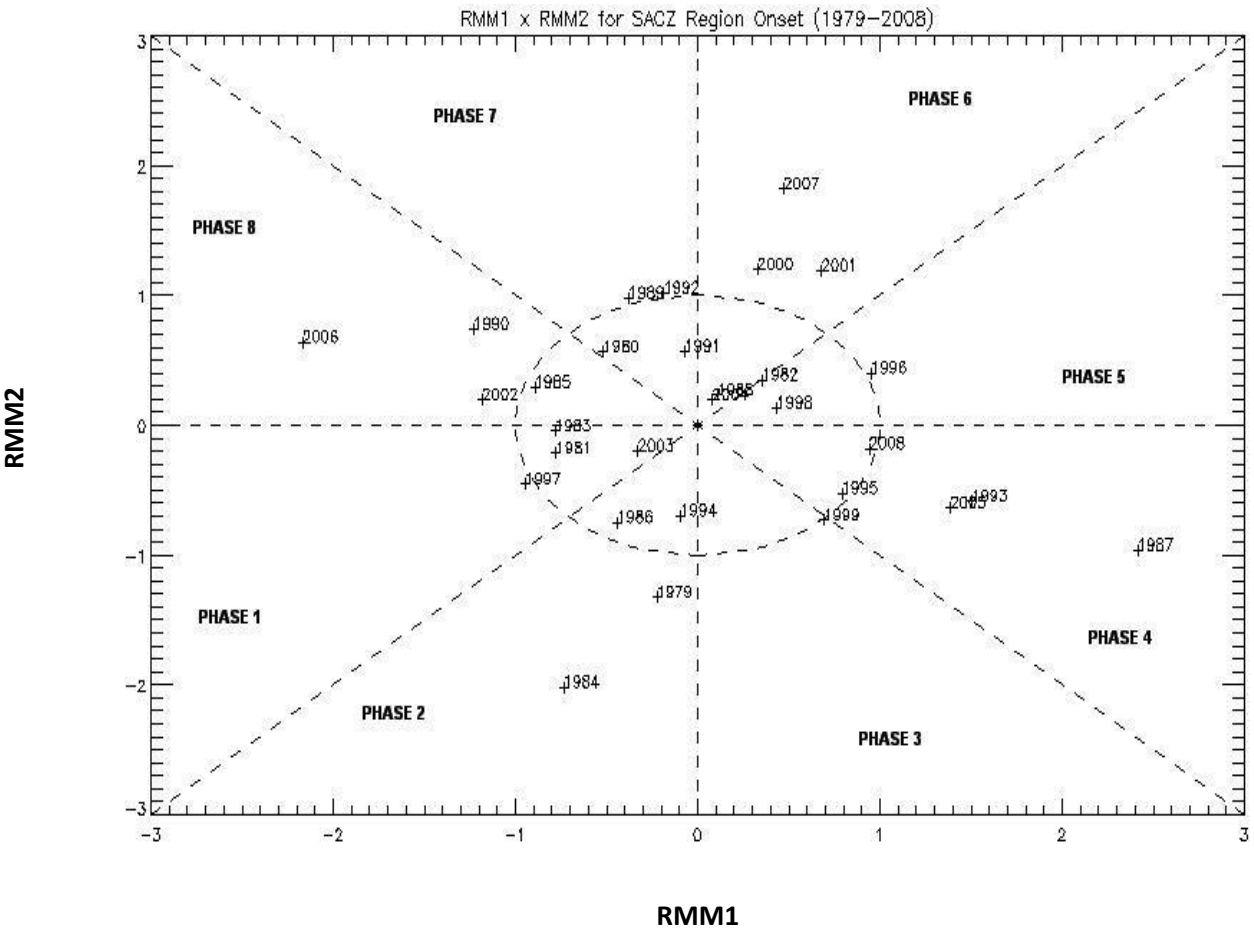

Figure 33: 1979-2008 SACZ Region Onset and MJO Phase Diagram

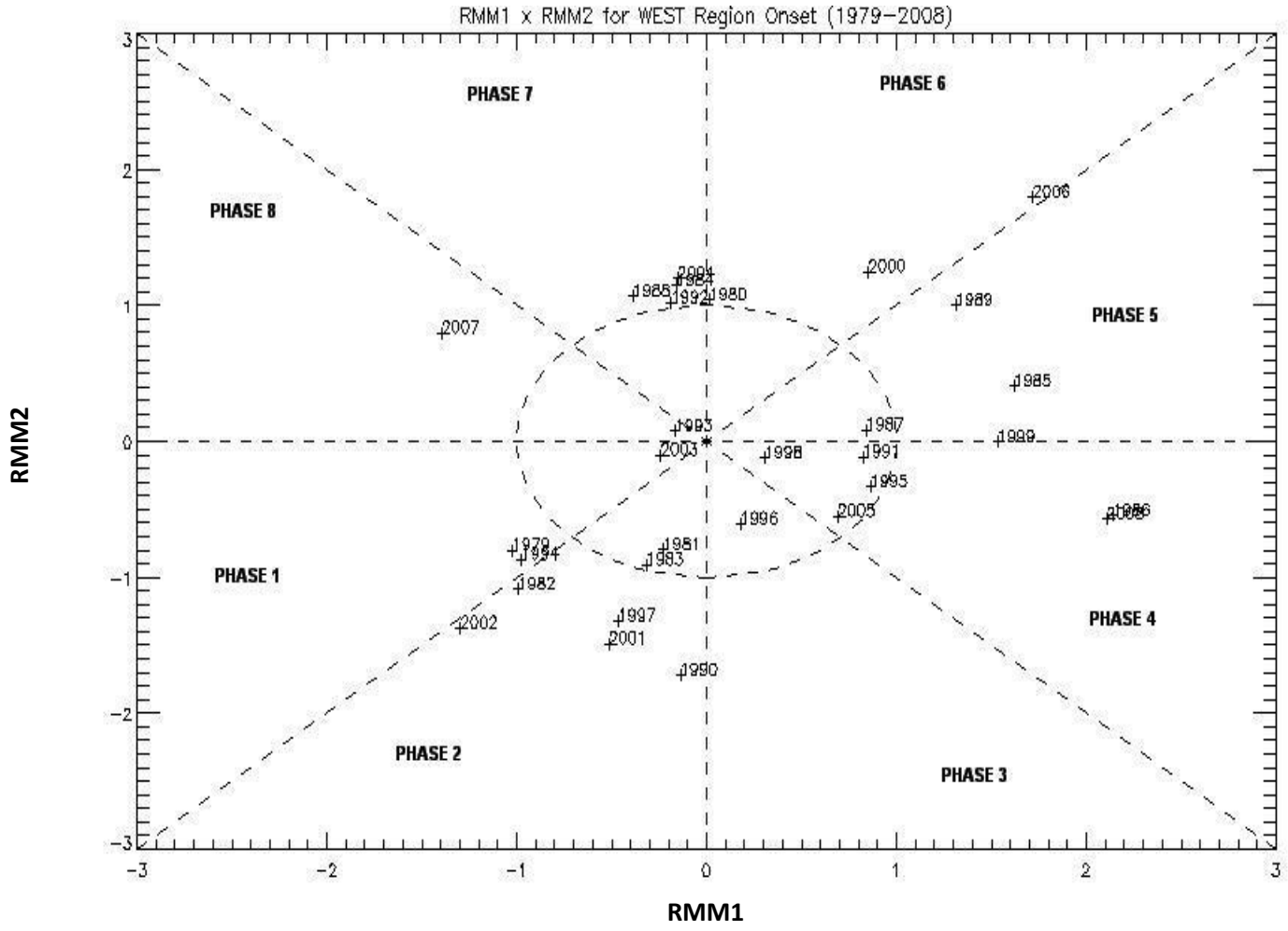

Figure 34: 1979-2008 West Region Onset and MJO Phase Diagram

5. CONCLUSIONS:

In this study, regional variability of monsoon onset in South America was analyzed using composites of GPCP rainfall and NCEP/NCAR Reanalysis upper and lower level variables. The study answered several questions, including how do cold fronts affect monsoon onset, and in what regions monsoon onset is affected by these cold fronts. Several of the precipitation composites confirm that monsoon onset occurs in the WR before the SACZ region. Therefore, the WR onset must occur before the SACZ region onset can occur. Onset for the WR is more related to the gradual change in atmospheric thermodynamic conditions before onset and the gradual increase in convection in the WR. This was confirmed by regional composites of thermodynamic conditions, as well as the analysis of volumetric soil moisture and heat fluxes. This was quantified in a lag correlation analysis, where potential temperature showed a 4 pentad lag between the WR and the SACZ meaning that potential temperature changed 4 pentads sooner than in the SACZ region. This analysis with the NCEP/NCAR reanalysis data, a completely independent of the GPCP rainfall data, verifies that there is a lag between the two regions and that the WR sees an increase in convection before the SACZ.

The SACZ region also requires certain thermodynamic conditions to be met in order for onset to occur, but there is more of a dynamical trigger needed to begin onset, based on the abruptness of the onset in the SACZ region. Cold fronts can affect the WR, which was shown in the normal, early, and late onset years time series for the WR, however they do not seem to be a large factor in the triggering of the onset as volumetric soil moisture, and sensible and latent heat fluxes still changed gradually before onset.

There are several differences in patterns between the “pre-onset” and “onset” cold fronts. For example, “pre-onset” cold fronts are shown to be stronger (based on stronger SLP and

temperature anomalies gradients) but do not bring precipitation to the SACZ region based on the "pre-onset" cold front composites for the SACZ region. "Pre-onset" cold fronts move quickly and cause strong temperature and SLP fluctuations, which was shown by the rapid progression of the "pre-onset" composite cold fronts that passed south of the SACZ region. "Onset" cold fronts extend into the SACZ region and bring precipitation to the region. Additionally, the precipitation associated with the "onset" stationary composite cold fronts verifies an abrupt onset in the SACZ region as cold fronts pass through the region during the "onset" composites but not in the "pre-onset" composites. At the time of onset, there is a radical change in the structure and propagation of cold fronts through South America. Therefore, cold fronts are causing onset in the SACZ region.

In looking at individual years where normal, early, and late onset occurred for the SACZ region and WR, there is a commonality between the variables studied that confirms the necessity for thermodynamic conditions to be met before onset can occur. An early onset year shows changes in thermodynamic conditions that favor monsoon onset much earlier in the year than in a late onset year. An earlier than normal change in latent heat flux and sensible heat flux signaled an early onset, and vice versa for a late onset. These changes are an outcome of the thermodynamics changes in the atmosphere at the time of the onset.

Additionally, the MJO and its influence on the variability of onset in the WR and the SACZ region were analyzed. Both the WR and the SACZ region had no onset dates within a strong suppressed convective phase of the MJO (phase 3). However, since phase 4, a documented suppressive phase of the MJO, did contain onset years for both the WR and the SACZ region, no conclusion can be made suggesting that the MJO can inhibit onset in these regions during a suppressive phase. The enhanced convective phases of the MJO cycle did not

significantly influence the variability of onset in the SACZ region either. We therefore conclude that the MJO does not have a significant effect on monsoon onset in the WR or SACZ regions.

This study confirmed the importance of cold fronts to the SACZ region, especially as they change at the time of onset. The transition of the cold front from "pre-onset" to "onset" suggests that the atmosphere within the SACZ region is changing at the time of onset, and that cold fronts are changing with it. In regards to early vs. late onset years, changes in heat fluxes are in response to convection increasing in the area. The earlier the fluxes change suggests an earlier onset year and vice versa. In addition, the variability of cold fronts and of thermodynamic conditions in the region confirms that there is regional variability within the WR and the SACZ region and a lag between the two regions. While this study finds that an abrupt change in the structure and propagation of cold fronts triggers monsoon onset in the SACZ region, the mechanism for those abrupt changes in cold fronts is left for future studies.

REFERENCES

Carvalho, L. M. V., C. Jones, and B. Liebmann, 2002: Extreme precipitation events in southeastern South America and large-scale convective patterns in the South Atlantic convergence zone. *J. Climate*, 15, 2377–2394.

Carvalho, L. M. V., C. Jones, and B. Liebmann, 2004: The South Atlantic convergence zone: Intensity, form, persistence, and relationships with intraseasonal to interannual activity and extreme rainfall. *J. Climate*, 17, 88–108.

Chen, T.C., S.P. Weng, and S. Schubert, 1999: Maintenance of Austral Summertime Upper-Tropospheric Circulation over Tropical South America: The Bolivian High–Nordeste Low System. *J. Atmos. Sci.*, 56, 2081–2100.

Fu, R., B. Zhu, and R.E. Dickinson, 1999: How Do Atmosphere and Land Surface Influence Seasonal Changes of Convection in the Tropical Amazon? *J. Climate*, 12, 1306–1321.

Grimm, A. M., and M. T. Zilli, 2009: Interannual Variability and Seasonal Evolution of Summer Monsoon Rainfall in South America. *J. Climate*, 22, 2257-2275.

Gallus, W. A., Jr., and M. Segal, 1999: Diabatic effects on Late Winter Cold Front Evolution: Conceptual and Numerical Model Evaluations. *Mon. Wea. Rev*., 127, 1518–1537.

Garreaud, René D, 2000: Cold Air Incursions over Subtropical South America: Mean Structure and Dynamics. *Mon. Wea. Rev.*, 128, 2544-2559.

Garreaud, R.D., and J.M. Wallace, 1998: Summertime Incursions of Midlatitude Air into Subtropical and Tropical South America. *Mon. Wea. Rev*., 126, 2713–2733.

Horel, J.D., 1984: Complex Principal Component Analysis: Theory and Examples. *J. Appl. Meteor*., 23, 1660–1673.

Huffman, G.J., R.F. Adler, M. Morrissey, D.T. Bolvin, S. Curtis, R. Joyce, B McGavock, J. Susskind, 2001: Global Precipitation at One-Degree Daily Resolution from Multi-Satellite Observations. *J. Hydrometeor*. 2, 36-50.

Jones, C., and L. M. V. Carvalho, 2006: Changes in the Activity of the Madden-Julian Oscillation during 1958-2004. *J. Climate*, 19, 6353-6370.

Kalnay et al., 1996: The NCEP/NCAR 40-year reanalysis project, *Bull. Amer. Meteor. Soc*., 77, 437-470.

Kousky, V. E,. 1988: Pentad Outgoing Longwave Radiation Climatology for the South American Sector. *Revista Brasileira de Meteorologia*, 217-231.

Lenters, J.D., and K.H. Cook, 1997: On the Origin of the Bolivian High and Related Circulation Features of the South American Climate. *J. Atmos. Sci.*, 54, 656–678.

Li, W., and R. Fu, 2006: Influence of Cold Air Intrusions on the Wet Season Onset over Amazonia. *J. Climate*, 19, 257–275.

Li, W., and R.Fu, 2004: The Influence of the Land Surface on the Transition from Dry to Wet Season in Amazonia. *Theor. Appl. Climatol.*78, 97-110.

Li, W., and R. Fu, 2004: Transition of the Large-Scale Atmospheric and Land Surface Conditions from the Dry to the Wet Season over Amazonia as Diagnosed by the ECMWF Re-Analysis. *J. Climate*, 17, 2637–2651.

Liebmann, B., J.A. Marengo, J.D. Glick, V.E. Kousky, I.C. Wainer, and O. Massambani, 1998: A Comparison of Rainfall, Outgoing Longwave Radiation, and Divergence over the Amazon Basin. *J. Climate*, **11**, 2898–2909.

Lupo, A.R., J.J. Nocera, L.F. Bosart, E.G. Hoffman, and D.J. Knight, 2001: South American Cold Surges: Types, Composites, and Case Studies. *Mon. Wea. Rev*., 129, 1021–1041.

Madden, R. A. and P. R. Julian, 1971: Detection of a 40–50 day oscillation in the zonal wind in the tropical Pacific. *J. Atmos. Sci.*, 28:702–708.

Marengo, J.A., B. Liebmann, V.E. Kousky, N.P. Filizola, and I.C. Wainer, 2001: Onset and End of the Rainy Season in the Brazilian Amazon Basin. *J. Climate*, 14, 833–852.

Nieto-Ferreira, R., T.M. Rickenbach, D.L. Herdies, and L.M.V. Carvalho, 2003: Variability of South American Convective Cloud Systems and Tropospheric Circulation during January–March 1998 and 1999. *Mon. Wea. Rev*., 131, 961–973.

Nieto-Ferreira, R. and T. M. Rickenbach, Regionality of monsoon onset in South America: A three-stage conceptual model. *Int. J. Clim.,* doi:10.1002/joc.2161, 2010.

Nogues-Paegle JN, Mo KC. 1997. Alternating wet and dry conditions over South America during summer. *Mon. Wea. Rev.* 125:279–291.

Raia, A., and I. Cavalcanti, 2008: The Life Cycle of the South American Monsoon System. *J. Climate*, 6227-6246.

Ramage, C. S., 1971: Monsoon Meteorology. *Academic Press*, 269 pp.

Rickenbach, T. M., R. Nieto-Ferreira, J. Rickenbach, and E. Wright, 2009: Monsoon in the Americas: Opportunities and challenges. *Geography Compass*, 3, 1-16.

Seluchi, M., Y.V. Serafini, and H. Le Treut., 1998: The Impact of the Andes on Transient Atmospheric Systems: A Comparison between Observations and GCM results. *Mon.Wea. Rev.*, 895-912.

Silva Dias, P.L., W.H. Schubert, and M. DeMaria, 1983: Large-Scale Response of the Tropical Atmosphere to Transient Convection. *J. Atmos. Sci.*, 40, 2689–2707.

Wheeler, M., and H. H. Hendon, 2004: An all-season real-time multivariate MJO index: Development of an index for monitoring and prediction. *Mon. Wea. Rev.*, 132, 1917–1932.

Zhou, J., and K.M. Lau, 1998: Does a Monsoon Climate Exist over South America? *J. Climate*, 11, 1020–1040.